6-2015

Design and Analysis of Speed Control Using Hybrid PID-Fuzzy Controller for Induction Motors

Ahmed Fattah
Western Michigan University, ahmed_kikan@yahoo.com

Follow this and additional works at: http://scholarworks.wmich.edu/masters_theses

Part of the Automotive Engineering Commons, and the Electrical and Computer Engineering Commons

Recommended Citation

DESIGN AND ANALYSIS OF SPEED CONTROL USING HYBRID PID-FUZZY
CONTROLLER FOR INDUCTION MOTORS

by

Ahmed Fattah

A thesis submitted to the Graduate College
in partial fulfillment of the requirements
for the degree of Master of Science in Engineering (Electrical)
Electrical and Computer Engineering
Western Michigan University
June 2015

Thesis Committee:

Ikhlas Abdel-Qader, Ph.D., Chair
Johnson Asumadu, Ph.D.
Abdolazim Houshyar, Ph.D.

DESIGN AND ANALYSIS OF SPEED CONTROL USING HYBRID PID-FUZZY
CONTROLLER FOR INDUCTION MOTORS

Ahmed Jumaah Fattah, M.S.E.

Western Michigan University, 2015

This thesis presents a hybrid PID-Fuzzy control system for the speed control of a

three-phase squirrel cage induction motor. The proposed method incorporates fuzzy logic

and conventional controllers with utilization of vector control technique. This method

combines the advantages of fuzzy logic controller and conventional controllers to

improve the speed response of the induction motor. The design of fuzzy system consists

of 9 fuzzy variables and 49 IF-THEN rules that define the behavior of the system. The

FLC observes the loop error signal and correspondingly control the PID input error signal

so that the actual speed signal matches the reference speed signal with reduced rise time,

settling time, and peak over shoot. Implementation and simulation results using

MATLAB/SIMULINK of various hybrid system controllers such as (PI-, PD-, and PID-

fuzzy) are compared along with conventional PI controller in terms of several

performance measurements such as rise time (tr), maximum percent overshoot (M_p),

settling time (ts), and steady state error (E_{ss}) at various load conditions. The results

verified the effectiveness of the proposed hybrid speed controller under different

operating conditions and demonstrated improvements in performance in speed tracking

and system's stability.

ACKNOWLEDGMENTS

I would like to express my deepest appreciation to my committee chair Professor Ikhlas Abdel-Qader for her guidance, enthusiastic encouragement and useful critiques of this research work. Without her supervision and constant help this thesis would not have been possible.

Besides my advisor, I would like to thank the members of my thesis committee: Professor Johnson Asumadu and Professor Abdolazim Houshyar for their time and their feedback on my work.

Additionally, I wish to thank my best friends for helping me get through the difficult times, and for all the emotional support, camaraderie, entertainment, and caring they provided.

Finally, and most importantly, I would like to express the profound gratitude from my deep heart to my beloved family: my parents Jumaah Fattah and Yusra Hameed, my wife Narmeen Jamal, my brothers, and my sisters. They were always supporting me and encouraging me spiritually throughout my life. Without their support, it is impossible for me to complete my college and graduate education seamlessly. To them I dedicate this thesis.

<div style="text-align:center">Ahmed Jumaah Fattah</div>

TABLE OF CONTENTS

Table of Contents—Continued

CHAPTER

LIST OF TABLES

LIST OF FIGURES

List of Figures—Continued

CHAPTER1

INTRODUCTION AND PERTINENT LITERATURE

1.1.   Introduction

Induction motors, particularly the squirrel cage induction motors (SCIM) as shown in figure 1.1 have been widely used in industry application such as hybrid vehicles, paper and textile mills, robotics, and wind generation systems because of their several inherent advantages such as their simple construction, robustness, reliability, low cost, and low maintenance needs. Without proper controlling, it is virtually impossible to achieve the desired task for any industrial application. [1].

Figure 1.1: Three phase squirrel cage induction motor [2].

Open loop control of induction motor (IM) with variable frequency and variable voltage amplitude provide a satisfactory variable speed motor for steady torque operation and without stringent requirements on speed regulation. However, for high performance drive requirements including fast dynamic response, accurate speed, and accurate torque

control of induction motor is a challenging problem due to their highly coupled nonlinear structure and many of the parameters vary with the operating conditions such as load torque, reference speed set point, rotor resistance, and motor temperature [3].

To achieve optimal efficiency of induction motors, several control techniques have been developed to control the induction motor such as scalar control, vector or field oriented control, direct torque control. Scalar control is one of the first control techniques of induction motors. In this method the ratio of both the amplitude and frequency of the supply voltage is kept constant in order to maintain a constant air gap flux and hence provide maximum torque. Scalar control drives are easy to implement but does not yield satisfactory results for high performance applications because of inherent coupling effects between torque and flux give sluggish response and system is easily prone to instability. This problem can be solved by field oriented control or direct torque control. In most of industrial drive control applications, the standard method to control induction motor is based on the field oriented or vector control principle in order to achieve the best dynamic behavior. In this method the decoupling between the flux and torque allows the induction motor to be controlled in a similar method to that in the control of separately exited dc motors. Therefore it can be used for high performance applications [4].

Over the years, the conventional control such as the proportional plus integral (PI), and proportional plus integral plus derivative (PID) controllers have been used together with vector control methods to better control the speed of induction motors. However, it must be pointed out that conventional controllers have major drawback such as performance sensitivity to variations in system's parameters, and the fact that when using fixed gains the controller may not provide the required speed performance under

variations in the motor parameters and operating conditions. In order to overcome these challenges, Fuzzy Logic controller (FLC) has been used for motor speed control [5].

The main advantage of fuzzy logic controller when compared to the conventional controller is that no mathematical model is required for the controller design. Fuzzy logic has been successfully used to control ill-known or complex systems where precise modeling is difficult or impossible [6]. It has been demonstrated that dynamic performance of electric drives as well as robustness with respect to parameter variations can be improved by adopting the nonlinear speed control techniques as in the ones fuzzy control provides [7] and [8]. Recently, hybrid control techniques based on combination of two or more control methods are proposed to enhance controller's performance. Our proposed method combine conventional controller with fuzzy logic controller and vector control technique to take advantage of the best attributes of both controllers and eliminate the drawbacks of conventional controller such as oscillation, overshoot, and undershoot and the drawback of FLC such as steady state error.

1.2. Literature Review

As mentioned in previous section, induction motors have been widely used in industry application. Therefore, much attention is given to their control for various applications with different control requirements. In recent years, intelligent control methods such as fuzzy control, neural network control, and hybrid control have been proposed to enhance the performance of induction motors [9]. Different control methods for speed control of induction motor are reviewed in the following literature survey:

Senthilkumar et al. [10] presented a PID controller for three phase induction motor using V/F method. The used control scheme is based on constant volts per hertz ratio and PID controller. The PID controller is designed to generate the signals in order to turn on six Insulated-Gate Bipolar Transistors (IGBT) of a three-phase inverter. In the conclusion, he proposed to extend the controller with other soft computing techniques.

Marwan et al. [11] proposed a fuzzy logic based speed control system for three phase induction motor using scalar control technique. The proposed controller design was simulated using MATLAB/SIMULINK software, and the performance of proposed system is analyzed with various operating conditions like different reference speed and change in load that applied to the motor. The result showed that FLC has faster response and better performance compared with PI controller.

Sharda et al. [6] investigated the use of FLC scheme for controlling induction motor parameters such as starting current, flux, torque, and speed. They reported results on two cases: 1) induction motor controlled by PI controller, in which the three phase currents, acceleration curve, and output torque are investigated, and 2) induction motor controlled by FLC, in which the same performance parameters have been investigated. They reported that the performance is improved regarding magnitude of starting currents and also time response of acceleration. For example, with PI controller the amplitude of starting current is 500 A and the rise time is 0.7 sec. While, with FLC the amplitude of starting current is 200 A and the rise time is 0.55 sec. These results show that FLC has improved the rise time with less starting current compared with PI controller.

A detailed comparison between scalar and indirect vector control techniques of induction motor are presented by Behera et al. [4]. The performance of PI based scalar control and PI based vector control are evaluated by showing the advantages and disadvantages of each control scheme. The results showed that it is very hard to design the control structure based PI controller because the system is influenced by unpredictable variations in the machine parameters. Robust control techniques were suggested to replace the PI controller to provide better control.

Amanulla et al. [8] proposed simple structured neural network based new identification method for flux position estimation, sector selection and stator voltage vector selection for induction motors using direct torque control method (DTC). In this method the drawbacks of DTC such as torque and flux ripple have been improved. The result support that artificial neural network based DTC has better performance than modified DTC.

A systematic approach of achieving robust speed control of an induction motor drive by means of Takagi-Sugeno based fuzzy control strategy has been investigated in [7]. The Takagi-Sugeno control strategy coupled with rule based approach in a fuzzy system yields more effective control design with improved system performance compared to the other methods.

Nitin et al. [12] demonstrated the performance analysis of three phase induction motor fed by SPWM inverter using different simulation technique in MATLAB/SIMULINK. The proposed system adjusts the amplitude and frequency of the stator voltage through voltage source inverter (VSI) combined with PI or FLC to control

the speed of the motor. Also, the results of FLC give better performance than PI controller.

1.3. Problem Statement

Induction motors are most widely used in all industries. The speed of the induction motor has to be varied according to application requirement. Therefore, there is a need for more efficient and reliable induction motor drive systems for current and future applications. Induction motors are highly non-linear systems, having uncertain time varying parameters mainly rotor resistance and subjected to unknown load disturbance. In addition, the rotor flux is inaccessible for state feedback control. Taking these difficulties into account, various control strategies are proposed such as vector control method, direct torque control, and sliding mode control. The use of proportional plus integral (PI) controller for speed control of induction motor with above mentioned techniques gives reasonable performance in steady state operation. However, this performance characterized by an overshoot, slow transient response, steady state error and the main drawbacks of this kind of controllers is its sensitivity to variation in system's parameters and the fact that when using fixed gains the controller may not provide the required speed performance under variations in the motor load torque and operating conditions. In order to overcome these challenges, hybrid PID-Fuzzy Logic controller has been proposed for induction motor speed control [3], [4], [13], and [14].

1.4. Scope and Objectives

The main objective of this work is to design a control method to provide optimal dynamic response of squirrel cage induction motor. This will be achieved by incorporate

fuzzy logic with conventional controllers and utilization of vector control technique. Implementation and simulation results using MATLAB/SIMULINK of various hybrid system controllers such as (PI-, PD-, and PID-fuzzy) are analyzed and compared along with conventional PI controller in terms of several performance measurements such as rise time (tr), overshoot (Mp), settling time (ts) and steady state error at various load conditions.

1.5.   Thesis Outline

This thesis is broke down into five chapters. Chapter II gives an introduction, principle, and detailed mathematical model of field oriented control. Additionally, a brief description of space vector projection in stationary and rotating reference frame and the transformation between them is given in this chapter. The background and structure of both conventional controllers and fuzzy controllers are presented in chapter III. Also, the design of hybrid fuzzy-PID controller is described. In chapter IV, the SIMULINK model is presented and simulation results for the proposed controller techniques are analyzed and compared under different operating conditions. Finally, the conclusion and recommendations for future work according to the work done are summarized in chapter V.

CHAPTER 2

FIELD ORIENTED CONTROL OF INDUCTION MOTOR

2.1.   Introduction

Vector control or field oriented control has invented by Blaschke [15] to emulate

DC motor characteristics in an induction motor [4] and [16]. In general, an electrical

motor can be thought of as controlled torque source. The torque is produce in the motor

by the interaction between the magnetic field of the stator field and the current in the

rotor. The stator field should maintain at a certain level, sufficiently high to produce a

high torque, but not too high to result in excessive saturation of the magnetic circuit of

the motor. By fixed stator field, the torque is proportional to the rotor current [17].

 The construction of a separately excited DC motor ensures that the stator field is

always orthogonal to the rotor field. Being orthogonal, there is no interaction between

these two fields. Therefore, independent control of the rotor current and stator field is

feasible where the current in the stator determine the system field, while the current in the

rotor can be used as a direct mean of torque control [4], [17] and [18].

In squirrel-cage induction motor, the rotor current is not fed directly by an

externally source but it result from induced e.m.f in the rotor winding. In other words, the

stator current is the source of magnetic field in the stator and rotor current. Therefore, the

control of induction motor is not simple as DC motor due to the interaction between the

stator field and rotor field whose orientation is not always held at 90° but it is varying

depending on the operation conditions. We can obtain DC motor like performance in an

induction motor by holding orthogonal orientation between the stator and rotor fields to achieve independently control of flux and torque. Such a scheme is called vector control or field oriented control [16] and [18]. First we will review the fundamentals of torque production and control in the DC motor.

2.2. Torque Control in DC Motor

A simplified representation of the DC motor is shown in figure 2.1. The magnetic circuit of the stator is represented by a pair of magnetic poles N and S, which represent the field part of the motor. Therefore, the space vector λ_f of flux linkage generated by the field winding is stationary and aligned with the d-axis of the stator. The commutator and properly positioned brushes ensure that the space vector I_a of the armature winding current is always aligned with the q-axis and 90° degree apart from λ_f space vector, even though the rotor is revolving. Therefore, these space vectors, which are stationary in space, are orthogonal or decoupled by nature [19].
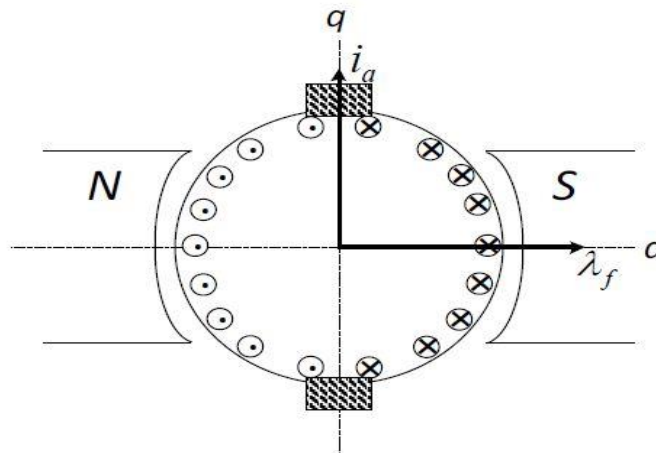
Figure 2.1: Simple representation of separately excited DC motor construction [19].

The induced e.m.f in the armature develops a torque that is proportional to the vector product of I_a and λ_f to the sine of angle between these vectors. As seen in figure 2.2, this is always a right angle which ensures the highest torque production. Therefore, the developed torque is given by

$$T_e = K_T I_f I_a \dots\dots\dots\dots\dots\dots\dots\dots\dots\dots\dots\dots\ 2.1$$

where I_a is the armature current (torque component), I_f is the field current (field component) which produces the flux linkage λ_f, and K_T is a constant dependent on the construction and size of the motor [19] and [20].
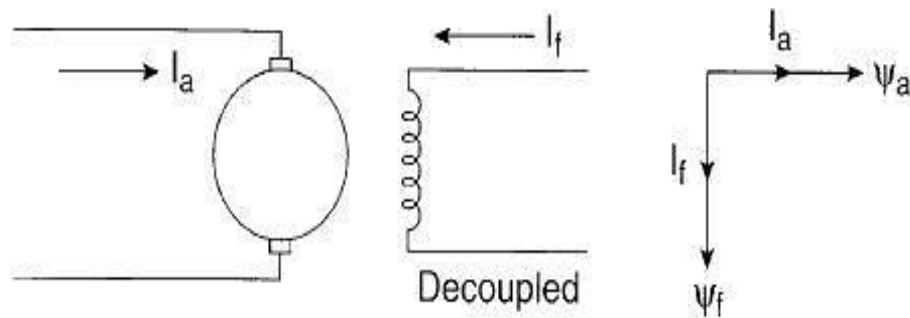
Figure 2.2: Separately excited DC motor and current space vector [20].

The flux linkage λ_f is not affected when the torque controlled by controlling the current I_a because of decoupling. Therefore, we get fast transient response. When the field current I_f is controlled, it impacts the field flux linkage λ_f only not armature's flux λ_a. Because of the inherently decoupling problem, an induction motor cannot generally give such fast response [19] and [20].

2.3.   Field Oriented Control Principle

Field oriented control (FOC) consists of controlling the stator current components, represented by a vector, in a synchronously rotating reference frame d^e-q^e, in which the expression of the electromagnetic torque of the smooth-air-gap of the motor is similar to the expression of the torque in a separately excited DC motor. This technique is based on transformation of three phase time and speed dependent system into two coordinate time variant system, where the sinusoidal variable appears as DC quantities in steady state. Thus, this transformation leads to a structure similar of that in DC motor [20], [21], and [22].

The motor terminal phase currents I_{as}, I_{bs}, and I_{cs} are converted by Clarke transformation from three-phase to two-phase sinusoidal signals, I_d^s and I_q^s components, as shown in figure 2.3a. The two components are then converted by Park transformation to I_d^e and I_q^e components. These components are the direct axis component and quadrature axis component, respectively, in the rotating reference frame as shown in figure 2.3b.

In FOC the direct component of stator current space vector I^e is analogous to field current I_f, and I_q^e is analogous to armature current I_a of a DC motor. Therefore, the torque can be expressed as

$$T_e = K_T I^e I_q^e \dots\dots\dots\dots\dots\dots\dots\dots\dots\dots\dots\dots 2.2$$

Or

$$T_e = \acute{K}_T \hat{\Psi}_r I_q^e \dots\dots\dots\dots\dots\dots\dots\dots\dots\dots 2.3$$

Where:

$\widehat{\Psi}_r$ is the peak value of sinusoidal space vector.

Te is the motor torque.

(a)

(b)
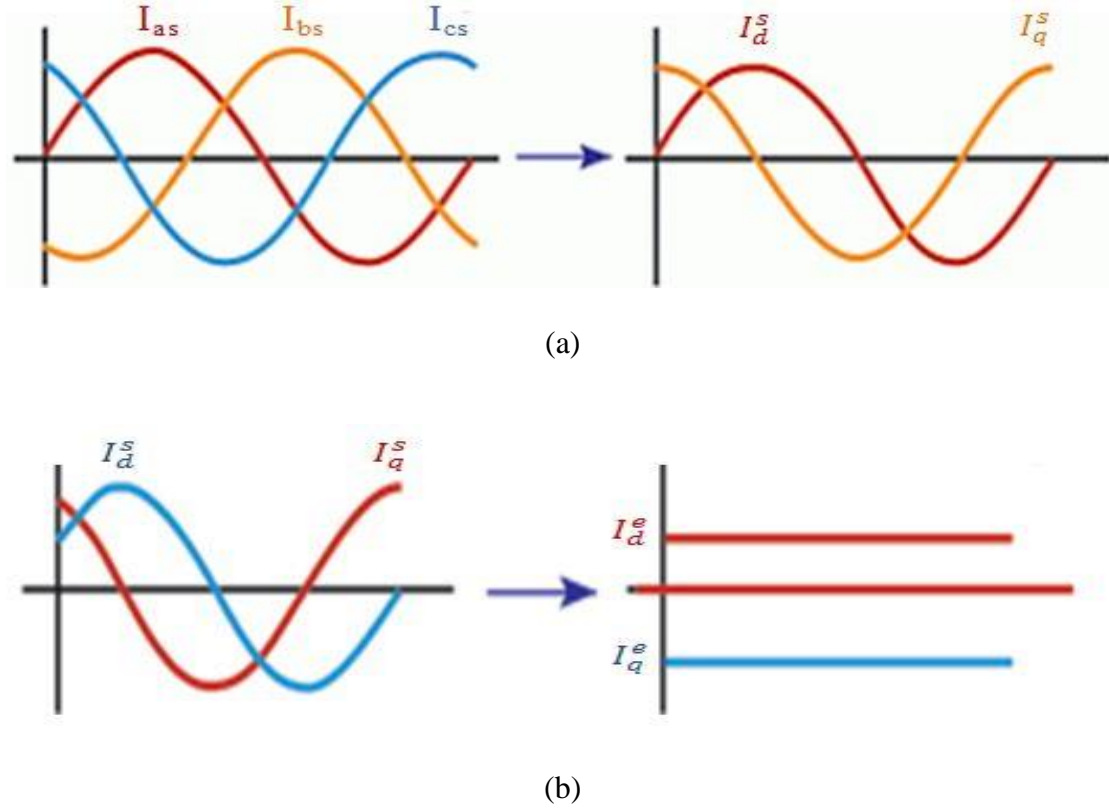
Figure 2.3: (a) Clarke transformations, (b) Park transformations.

The DC like machine performance can be achieved if the I_d^e is aligned in the direction of flux $\widehat{\Psi}_r$ and I_q^e is established perpendicular to it, as shown in figure 2.4. This mean that when quadrature reference current I_q^{e*} is controlled, it affects the actual I_q^e component only, but does not affect the flux $\widehat{\Psi}_r$. Similarly, when direct reference current I_d^{e*} is controlled, it controls the flux only and does not affect the I_q^e component of current.

This vector or field orientation of currents is essential under all operating conditions in a vector control drive [20].
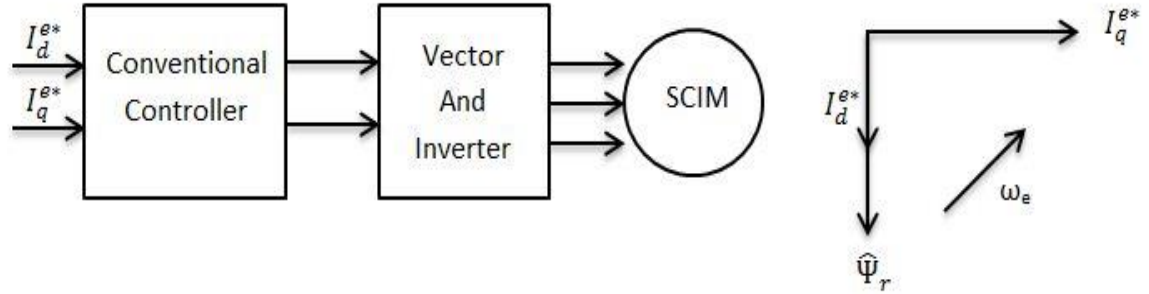
Figure 2.4: Vector control block diagram with two control current inputs.

2.4.   Space Vector Projection in Stator Reference Frame

The three-phase currents, voltage, and fluxes of AC motor can be analyzed in terms of complex space vector. Figure 2.5 shows a cross section of a simple three-phase, two pole AC motor with three-phase current vectors.
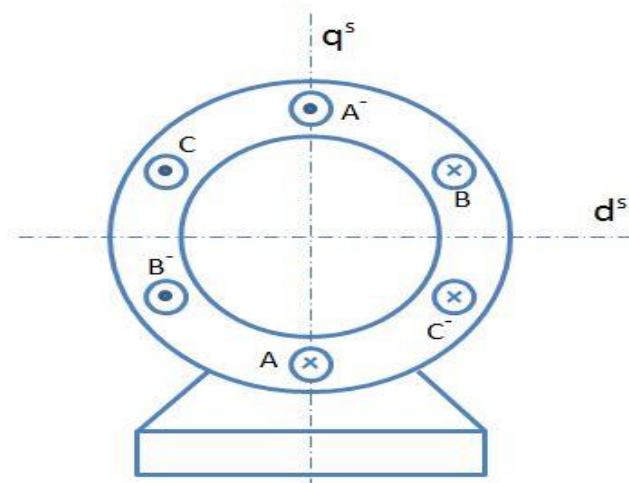
Figure 2.5: Schematic representation of a three-phase, 2-pole stator of an AC motor [17].

The horizontal and vertical geometrical axes of the stator are aligned with two axes, the direct axis, d^s, and the quadrature axis, q^s, respectively. They represent so-called stator or stationary reference frame.

The stator coils are supplied from a balanced three-phase AC source with a radian frequency ω. Figure 2.6 shows stator current vectors I$_{as}$, I$_{bs}$, and I$_{cs}$ at an instant of time, for example ωt=60°. The resultant stator current space vector, I$_s$, constitutes a vector sum of the phase currents vectors. Since the three currents are 120° apart from each other, and since the phase-A coil was assumed to be in the vertical axis of the stator, then, in analytical form,

$$I_s = I_{as}e^{j0} + I_{bs}e^{j120} + I_{cs}e^{j240} \ldots\ldots\ldots\ldots\ldots\ldots\ldots 2.4$$

It must be stressed that space vector has constant magnitude and rotate with angular velocity ω equal to the supply radian frequency [17].
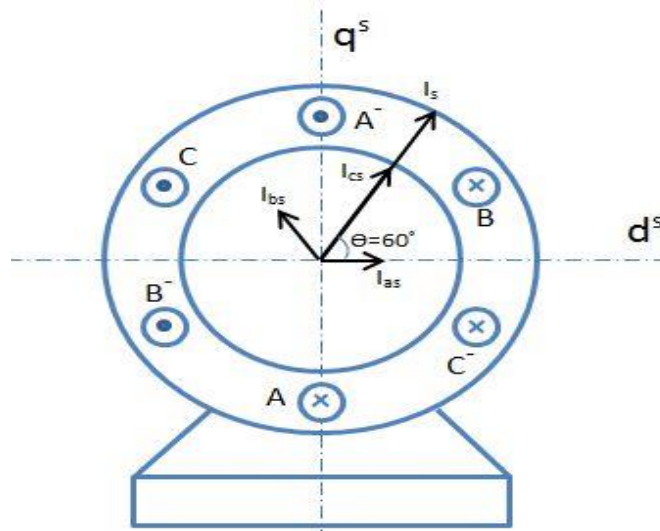
Figure 2.6: Stator current vectors at Θ = 60° [17].

Taking the d^s-axis as real and the q^s-axis as imaginary, vector $\vec{I_s}$ can be expressed as

$$\vec{I_s} = I_s\, e^{j\Theta} = I_d^s + jI_q^s \quad \dotsb \quad 2.5$$

Where, In a P-pole stator of an AC motor the geometrical angle, Θ, can be expressed as

$$\Theta = \frac{2}{P}\, \omega t \quad \dotsb \quad 2.6$$

And as illustrated in Figure 2.7, I_s donates the magnitude of vector $\vec{I_s}$, while I_d^s and I_q^s are its real part (d^s-axis) and imaginary (q^s-axis) components. This components have AC wave form under sinusoidal steady state conditions, this is because the current space vector is rotating vector with respect to the stator reference frame [17].
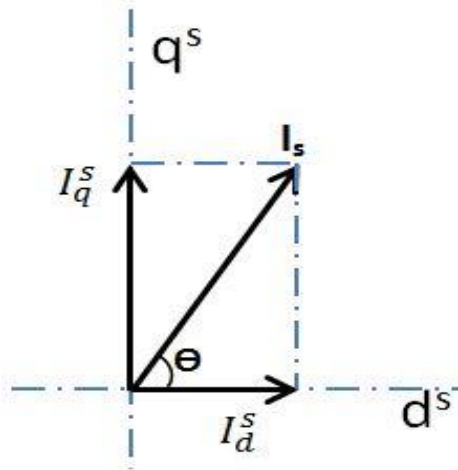
Figure 2.7: Stator current space vector and components in the stator reference frame [17].

2.5.   Space Vector Projection in Rotating Reference Frame

Control systems are usually represented by block diagrams in which the variables are time varying DC signals. Thus, Controlling AC motor is somewhat inconvenient

15

because of AC quantities. Therefore, another transformation will be needed to convert the AC d^s-q^s components of the motor into DC variables. This conversion is so-called excitation or rotating reference frame d^e-q^e [17].

The excitation reference frame rotates with the angular velocity ω in the same direction as the rotor flux space vector rotates. As a result, in the steady states, the motor vectors coordinates in the new reference frame don't vary in time. Figure 2.8 shows the stator current space vector in both stator reference frame and excitation reference frames [17].
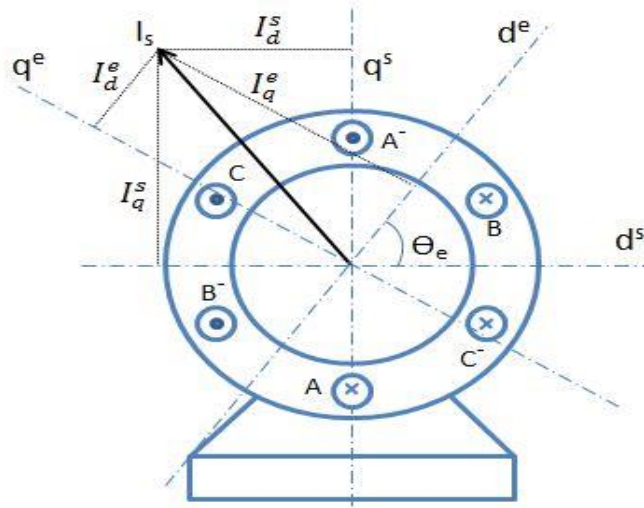
Figure 2.8: Stator current space vector and components in both the stator and excitation reference frame.

2.6. Forward and Inverse Clarke Transformation

The Clarke transformation converts a three-phase signals such as currents, voltage, and flux from three-phase coordinate system (a, b, c) into a two-phase coordinate orthogonal system (d^s, q^s). Figure 2.9 shows the graphical construction of the current space vector and its projection into stator reference frame (d^s, q^s). Where, the real part of

the current space vector is equal to instantaneous value of the direct-axis current

component I_d^s and imaginary part is equal to the quadrature-axis current component I_q^s

[17] and [23].
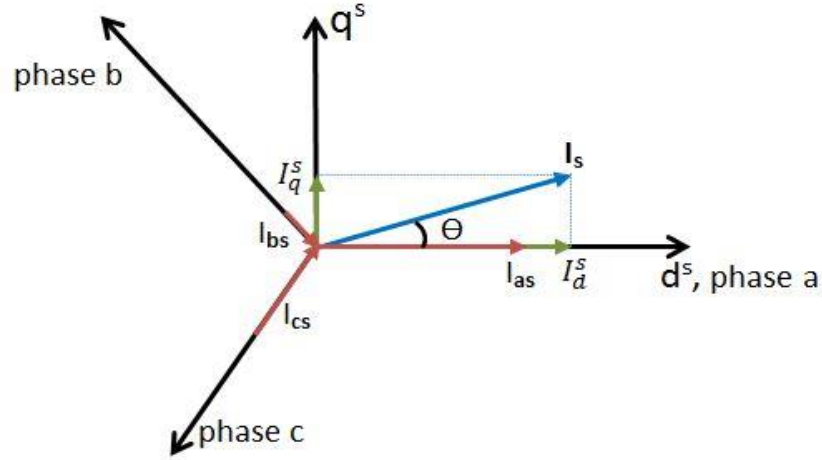
Figure 2.9: Stator current space vector and its component in the stationary
reference frame [23].

Assuming that the a-axis and d^s-axis are in the same direction, the quadrature-

phase stator current components I_d^s and I_q^s can be expressed in term of the instantaneous

values of the actual phase currents as:

$$\begin{bmatrix} I_d^s \\ I_q^s \end{bmatrix} = \begin{bmatrix} 1 & -\frac{1}{2} & -\frac{1}{2} \\ 0 & \frac{\sqrt{3}}{2} & -\frac{\sqrt{3}}{2} \end{bmatrix} \begin{bmatrix} I_{as} \\ I_{bs} \\ I_{cs} \end{bmatrix} \dots\dots\dots\dots\dots\dots\dots\dots\dots\dots\dots\dots\dots\dots\dots\dots 2.7$$

Where:

I$_{as}$, I$_{bs}$, and I$_{cs}$ are the actual stator currents

I^s, I_q^s are the direct and quadrature currents respectively [23].

The quadrature-phase stator current components I_d^s and I_q^s can be easily converted

from a two-phase coordinate orthogonal system (d^s, q^s) into a three-phase coordinate

17

system (a, b, c) by using the inverse Parke transformation. The matrix equation is expressed as [17]:

$$\begin{bmatrix} I_{as} \\ I_{bs} \\ I_{cs} \end{bmatrix} = \frac{2}{3} \begin{bmatrix} 1 & 0 \\ -\frac{1}{2} & \frac{\sqrt{3}}{2} \\ -\frac{1}{2} & -\frac{\sqrt{3}}{2} \end{bmatrix} \begin{bmatrix} I_d^s \\ I_q^s \end{bmatrix} \quad \dots\dots\dots\dots\dots\dots\dots\dots\dots\dots\dots\dots\dots\dots \text{ 2.8}$$

2.7. Forward and Inverse Park Transformation

Park transformation is the most important transformation in the field oriented control. It converts a two-phase orthogonal system (d^s, q^s) into rotating reference frame (d^e-q^e) [21]. Current space vector equations can be formulated in a rotating reference frame that rotates at a synchronous speed ω in the same direction as does the stator current space vector. As a result, in the steady state, coordinates of the stator current components in the new reference do not vary in time [17] and [23].

In rotating reference frame d^e-q^e the direct and quadrature axes (d^e and q^e) rotate at synchronous speed ω, as shown in figure 2.10, where Θ_e is the angle between the d^s-axis of the stationary reference frame and the d^e-axis of the rotating reference frame [23]. If the d^e-axis is aligned with the rotor flux vector, the transformation is expressed as

$$\begin{bmatrix} I_d^e \\ I_q^e \end{bmatrix} = \begin{bmatrix} \cos\Theta_e & \sin\Theta_e \\ -\sin\Theta_e & \cos\Theta_e \end{bmatrix} \begin{bmatrix} I_d^s \\ I_q^s \end{bmatrix} \quad \dots\dots\dots\dots\dots\dots\dots\dots\dots\dots\dots\dots\dots \text{ 2.9}$$

Where:

I_d^s, I_q^s are the direct and quadrature currents respectively in stationary reference frame

I_d^e, I_q^e are the direct and quadrature currents respectively in rotating reference frame [23].
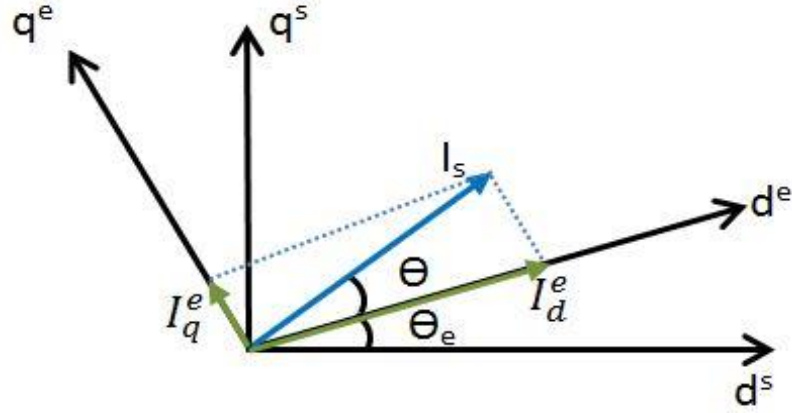
Figure 2.10: Stator current space vector and its component in the rotating reference frame [23].

While the inverse transformation from rotating reference frame to stationary reference frame is expressed as

$$\begin{bmatrix} I_d^s \\ I_q^s \end{bmatrix} = \begin{bmatrix} \cos\Theta_e & -\sin\Theta_e \\ \sin\Theta_e & \cos\Theta_e \end{bmatrix} \begin{bmatrix} I_d^e \\ I_q^e \end{bmatrix} \quad \cdots\cdots\cdots\cdots\cdots\cdots\cdots\cdots\cdots\cdots\cdots\cdots\cdots\cdots\cdots\cdots \text{ 2.10}$$

2.8.   Field Oriented Control Methods

Knowledge of the instantaneous rotor flux position (angle), with which the revolving reference frame is aligned, constitutes the necessary requirement for proper transformation from stationary reference frame to rotating reference frame, or vice versa, in field orientation. In fact if there is an error in this variable, the d^e-axis is not aligned with the rotor flux vector. Thus, I_d^e and I_q^e are incorrect flux and torque components of the stator currents [21].

There are two general methods to measure the rotor flux vector angle. One, called the direct or feed-back method was invented by Blaschke, and the other, known as the indirect or feed-forward method was invented by Hasse. The two methods differ in the way the rotor angle is determined [16].

19

2.9. Direct Field Oriented Control

In direct field oriented control (DFOC), the angle and magnitude of the reference flux vector are either measured or estimated from the stator currents and voltage using flux observers. Figure 2.11 shows a simple scheme for estimation the magnitude and phase (position) of the rotor flux vector, based on measuring the air gap flux and stator current. Placing two Hall sensors of magnetic field in the air gap of the motor, allows determination of the direct and quadrature components, λ_{dm} and λ_{qm}, of the air gap flux vector, λ_m. In analytical form, the rotor flux vector can be expressed as

$$\lambda_r = \frac{L_r}{L_m} \lambda_m - L_{1r} I_s \dots\dots\dots\dots\dots\dots\dots\dots\dots \quad 2.11$$
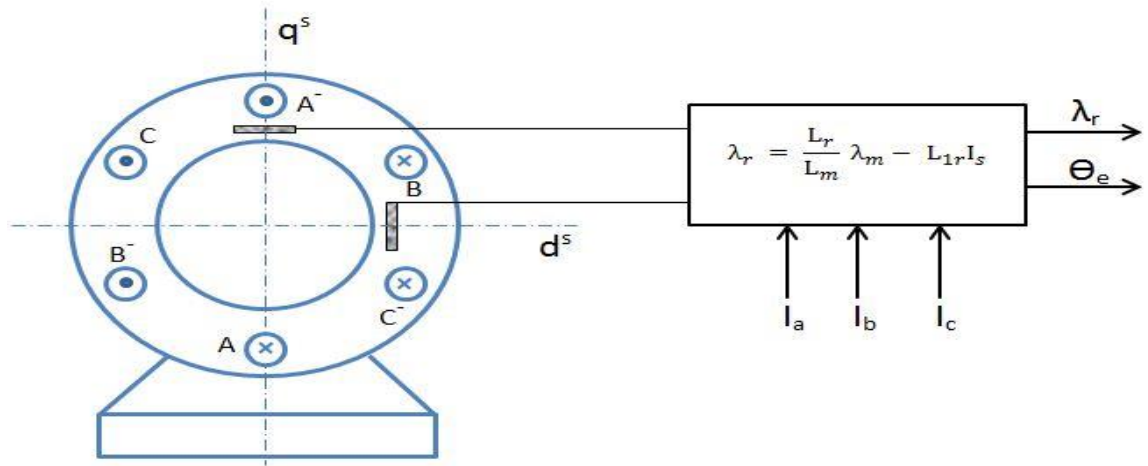
Figure 2.11: Determination of the magnitude and position of the rotor flux vector using Hall sensors and a rotor flux calculator [17].

Using equation (2.11), signals λ_{dr} and λ_{qr} calculated as

$$\lambda_{dr} = \frac{L_r}{L_m} \lambda_{dm} - L_{1r} I_d^s \dots\dots\dots\dots\dots\dots\dots\dots \quad 2.12$$

$$\lambda_{qr} = \frac{L_r}{L_m} \lambda_{qm} - L_{1r} I_q^s \dots\dots\dots\dots\dots\dots\dots\dots \quad 2.13$$

Magnitude, λ_r, and phase, Θ_e, of the rotor flux vector are determined using the rectangular to polar coordinate transformation [17], [19].

$$\lambda_{dr} + j\lambda_{qr} \xrightarrow{\text{yiels}} \lambda_r \angle \Theta_e \ \dots\dots\dots\dots\dots\dots\dots\dots\dots 2.14$$

Installing sensors in the air gap are inconvenient, and they spoil the ruggedness of the induction motor. Therefore, the stator current and voltage are using to compute the rotor flux vector. The stator flux vector can be estimated using following equation

$$\lambda_s = \int_0^t (\lambda_s - R_s I_s)\, dt + \lambda_s(0) \ \dots\dots\dots\dots\dots\dots\dots\dots 2.15$$

The air gap flux using the following equation

$$\lambda_m = \lambda_s - L_{1s} I_s \dots\dots\dots\dots\dots\dots\dots\dots 2.16$$

And the rotor flux vector, λ_r, can be estimated from equation (2.11) [19].

2.10.   Indirect Field Oriented Control

Indirect field orientation (IFO) is an alternative approach to direct flux orientation. It is based on calculation of the slip speed ω_r. The angular position, Θ_e, of the rotor flux vector is expressed as

$$\Theta_e = \int_0^t \omega_{sl}\, dt + \omega_{act}\, dt \ \dots\dots\dots\dots\dots\dots\dots 2.17$$

Where ω_{act} is the rotor speed, which is easy to measure using a shaft position sensor. And ω_{sl} is the slip frequency speed. The required value of slip speed can be calculated by following equation

$$\omega_{sl} \; = \; \frac{L_m}{L_r} \cdot \frac{R_r}{\hat{\Psi}_r} \cdot I_q^e \dots\dots\dots\dots\dots\dots\dots\dots \; 2.18$$

The IFO is more popular than DFO in industrial application due to implementation simplicity [17] and [19].

2.11. Indirect Field Oriented Control Algorithm

The block diagram of indirect field oriented control method is shown in figure 2.12. The induction motor is fed by a variable voltage, variable frequency PWM inverter, which operates in current control mode. The control scheme generates inverter switching commands to achieve the desired torque at the motor shaft. The algorithm of IFOC is given as:

1. Measure the stator phase currents I_a, I_b, and I_c. These currents are feed to Clarke transformation module that gives two components, $I_d{}^s$ and $I_q{}^s$, in stationary reference frame.

2. Transform the set of these two currents, I_d^s and I_d^s, into rotating reference frame. This conversion called Park transformation, and provides I^e and I_q^e.

3. The rotor flux is computed by

$$\hat{\Psi}_r \; = \; \frac{L_m I_d^e}{1+\tau_r} \dots\dots\dots\dots\dots\dots\dots\dots \; 2.19$$

Where τ_r is the rotor time constant calculated by

$$\tau_r = \frac{L_r}{R_r} \dots\dots\dots\dots\dots \; 2.20$$

4. The rotor angle, Θ_e, required for coordinate transformation is computed by equation (2.17).
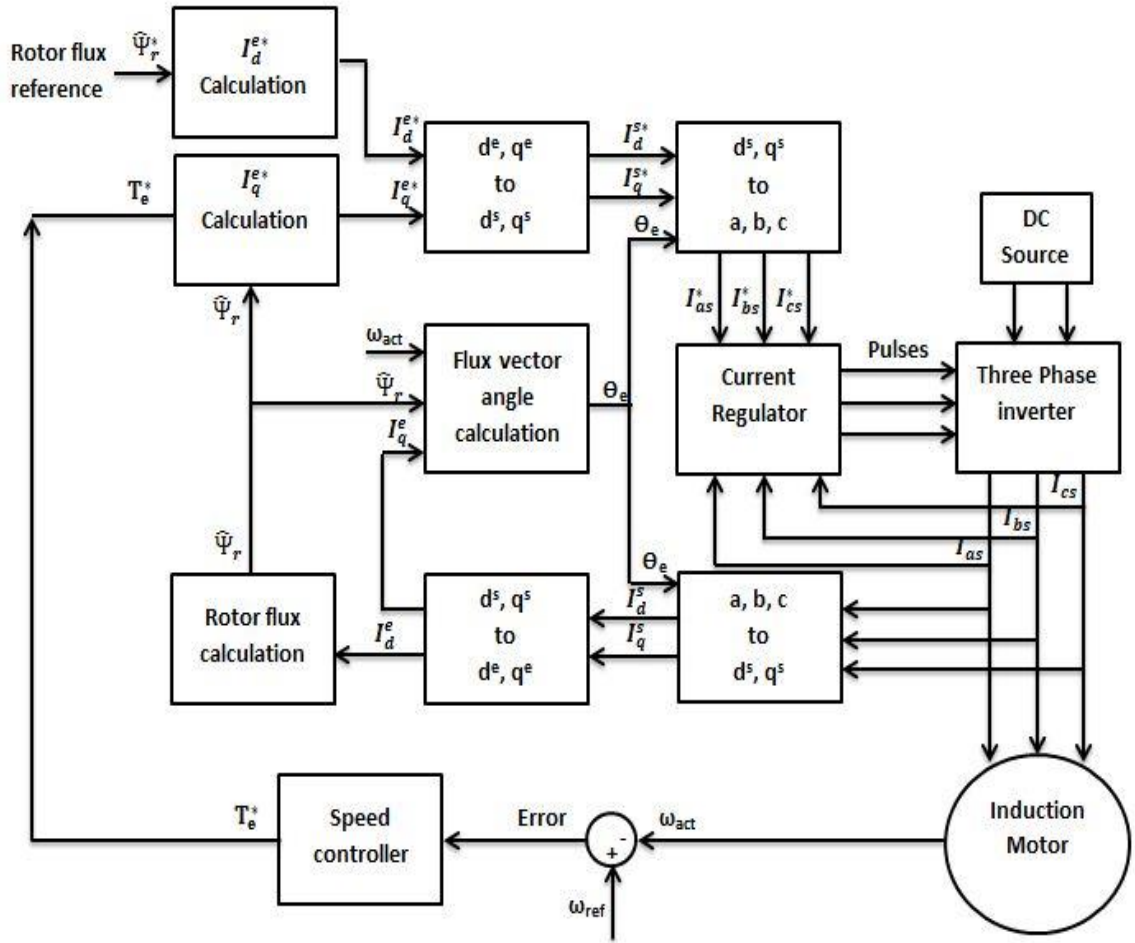
Figure 2.12: Indirect field oriented control scheme.

5. The motor speed, ω_{act}, is compared with the reference speed ω_{ref} and the error produced is fed to the speed controller. The output of the speed controller is electromagnetic torque T_e^*.

6. The quadrature stator current component reference I_q^{e*} is calculated by

$$I_q^{e*} = \left(\frac{2}{3}\right)\left(\frac{2}{p}\right)\left(\frac{L_r}{L_m}\right)\left(\frac{T_e^*}{\hat{\Psi}_r}\right) \dotfill 2.21$$

7. The direct stator current component reference I^{e*} is obtained by

$$I^{e*} = \frac{\hat{\Psi}_r^*}{I_m} \dotfill 2.22$$

8. I^{e*} and I_q^{e*} current references are converted into I_d^s and I_q^s, current references in stationary reference frame by using inverse Park transformation.

9. I^{s*} and I_q^{s*} current references are converted into phase current references I_a^*, I_b^*, and I_c^* by using inverse Clarke transformation and fed to the current controller. The controller processes the measured and reference currents to produce the inverter gating signals [18] and [24].

CHAPTER 3

THE DESIGN OF HYBRID SPEED CONTROLLERS

The dynamic d-q model of an AC motor is complex, multivariable, and nonlinear. However, vector control or field oriented control can overcome this problem, but accurate vector control is nearly impossible. To combat this problem, classical control, fuzzy logic controller, and hybrid fuzzy-PID controller are combined with indirect field oriented control to solve this problem [20].

3.1.   Conventional Controller

Induction motor can be controlled with the help of conventional PI, PD, and PID controller with the use of indirect field oriented control technique. The conventional controller is a feedback controller. It calculates an error value as the difference between the measured process value and the desired set point value and then drives the controlled plant to keep the steady state error equal to zero.

3.1.1   PI Controller

Proportional-Integral, PI, controller is most widely adopted in industrial application due to its simple structure, easy to design and low cost. PI controller produces an output signal consist of a sum of error and the integral of that error. The error represents the difference between the desired motor speed and the actual motor speed and it is expressed as

$$E = \omega_{ref} - \omega_{act} \ldots\ldots\ldots\ldots\ldots\ldots\ldots\ldots 3.1$$

Figure 3.1 shows the block diagram of classical PI controller. The transfer function for PI controller is expressed as

$$\frac{U(s)}{E(s)} = K_P + \frac{K_i}{s} \quad\ldots\ldots\ldots\ldots\ldots\ldots\ldots\ldots\ldots\ldots \quad 3.2$$

where K_P is the proportional gain, K_i is the integral gain, and U(s) is the output control signal which represent T_e^* torque reference in vector control drive.

Figure 3.1: PI controller block diagram with vector control.

The control signal is proportional to the error signal, the integral of error, the proportional gain K_p, and the integral gain K_i. The proportional controller will have the effect of reducing the rise time and steady state error. But, will never eliminate the error. The Integral control will have the effect of reduced the error near to zero value. But, it has a negative effect on the speed of the response and overall stability of the system.

3.1.2   PD Controller

Proportional-Derivative, PD, controller has the ability to predict the future error of the system. Therefore, it uses to increase the stability of the system. The output of PD controller consists of a sum of two terms, the error signal and the derivative of that error.

26

The error signal is computed by equation (3.2). Figure 3.2 shows the block diagram for

PD controller. The transfer function of PD controller is expressed as

$$\frac{U(s)}{E(s)} = K_P + K_d S \dots\dots\dots\dots\dots\dots\dots\dots\dots 3.3$$

Where K_P is the proportional gain, K_d is the derivative gain, and U(s) is the output control

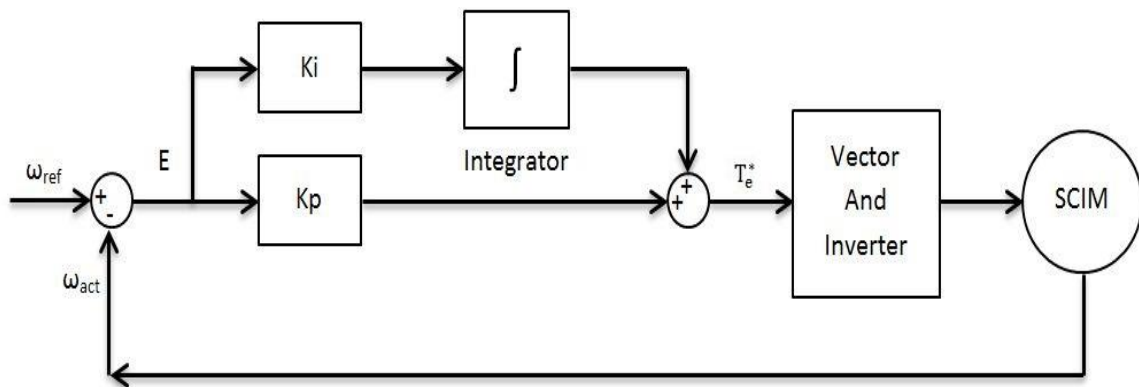signal which represent T_e^* torque reference in vector control drive.
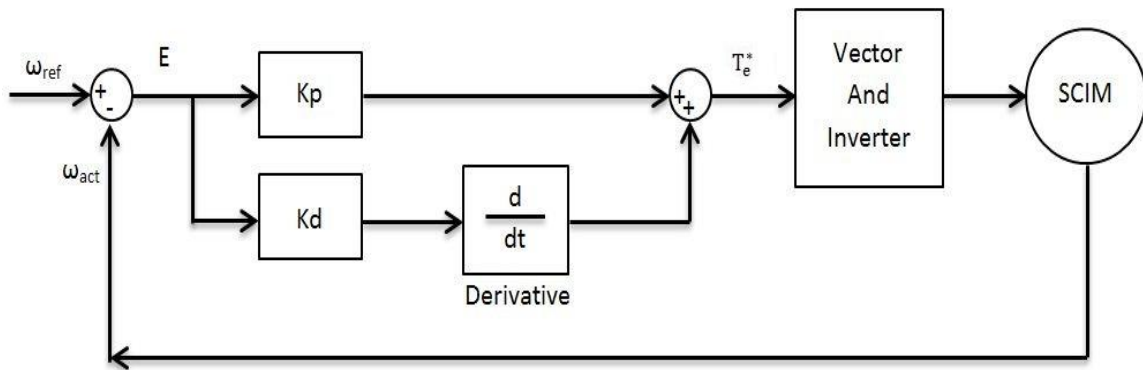
Figure 3.2: PD controller block diagram with vector control.

The control signal is proportional to the error signal, the derivative of the error,

the proportional gain K_i and the derivative gain K_d. Derivative control is used to

anticipate the future behavior of the error signal by using corrective actions based on the

rate of change in the error signal. Thus, it will have the effect of increasing the stability of

the system, reducing the overshoot, and improving the transient response.

3.1.3   PID Controller

Proportional-Integral-Derivative, PID, controller is widely used in industrial

control system. PID controller has all the necessary dynamics: fast reaction on change of

the controller input (D controller), increase in control signal to lead error towards zero (I

controller) and suitable action inside control error area to eliminate oscillations (P

controller). Derivative mode improves stability of the system and enables increase in gain

K$_p$, which increases speed of the controller response. The output of PID controller

consists of three terms the error signal, the error integral and the error derivative. The

error signal is computed by equation (3.2). Figure 3.3 shows the block diagram of PID

controller. The transfer function of PID controller is expressed as

$$\frac{U(s)}{E(s)} = K_P + \frac{K_i}{s} + K\ S \ldots\ldots\ldots\ldots\ldots\ldots\ 3.4$$

Where K$_P$ is the proportional gain, K$_d$ is the derivative gain, k$_i$ is the integral gain, and

U(s) is the output control signal which represent T$_e^*$ torque reference in vector control
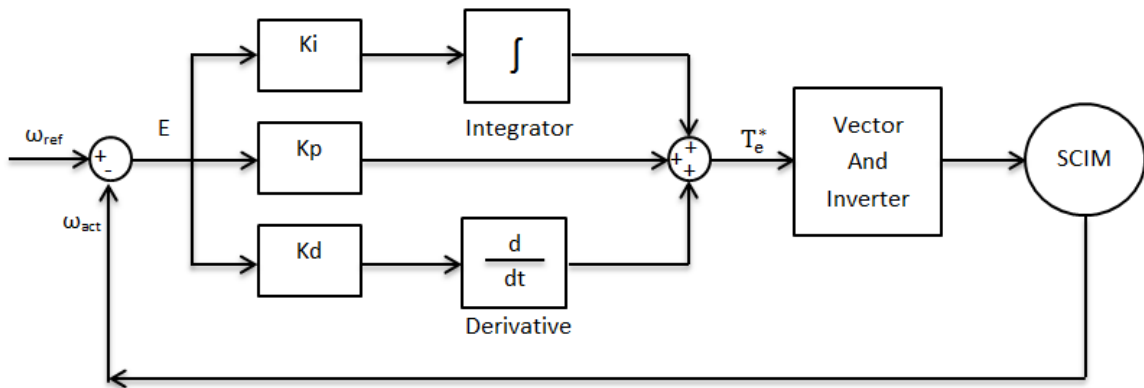
drive.

Figure 3.3: PID controller block diagram.

PID controller combines the advantage of proportional, derivative and integral

control action. Table 3.1 shows the effect of gain coefficient on the system performance.

28

Type	Rise time	Overshoot	Settling time	Steady state error
K_p	Decrease	Increase	Small change	Decrease
K_i	Decrease	Increase	Increase	Eliminate
K_d	Small change	Decrease	Decrease	Small change

Table 3.1: The effects of gain coefficients on the performance of PID controller system.

3.2.   Fuzzy Logic Controller

Fuzzy logic, FL, is another class of artificial intelligence. Its goal is planting human intelligence in a system so that the system can think intelligently like a human being [20]. Fuzzy logic techniques have been recognized in recent years as powerful tools for dealing with the modeling and control of complex systems for which no easy mathematical descriptions can be provided [3].

Fuzzy logic control is considered as a linguistic control strategy based on the use of if-then statement for the control process. In this statement, several variables that are expressed in natural English language such as positive, zero, and negative could be used either in antecedent (the if-part of the statement) or in consequent (the then-part of the statement). As a result, the mathematical model of the system is not required in fuzzy control so it can be applied to nonlinear systems [6].

3.2.1   Fuzzy Membership Function

Membership function MF is a curve that defines how the values of a fuzzy variable in a certain region are mapped to a membership value μ (degree of membership) between 0 and 1. Membership function can have different shapes such as triangular,

trapezoidal, Gaussian, and generalized bell as shown if figure 3.4. The most commonly used MF is the triangular type, which can be symmetrical or asymmetrical in shape [20].

(a)   (b)

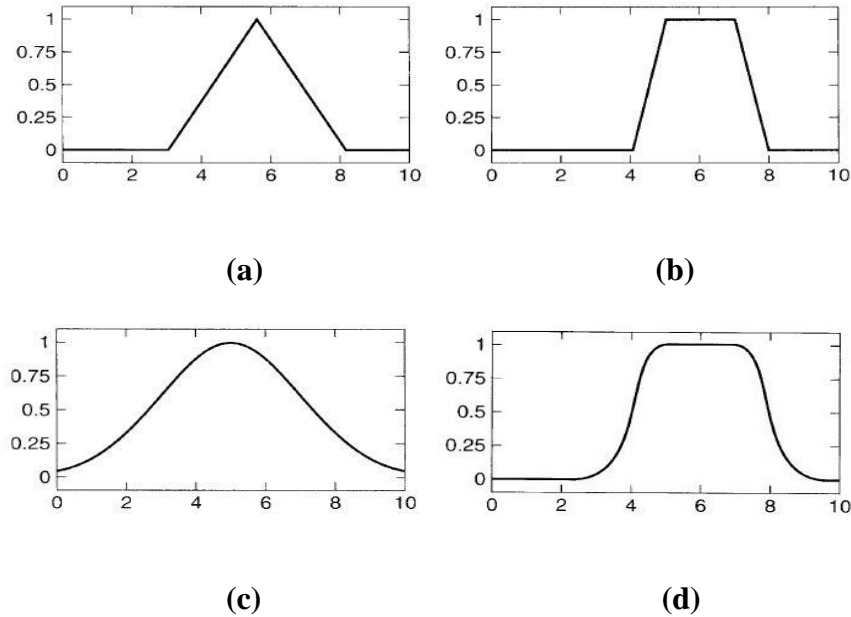(c)   (d)

Figure 3.4: Different types of membership functions (a) triangular (b) trapezoidal (c) Gaussian (d) generalized bell [20].

3.2.2   Fuzzy System Structure

The basic structure of fuzzy logic controller system is consist of four main part as shown in figure 3.5, which can be illustrated as follow [11]:

1. Knowledge base

    The Knowledge base is composed of data base and rule base. Data base consist of input and output membership functions that provides information for appropriate fuzzification and defuzzification operations. The rule base contains a set of linguistic rules that provide information for the inference engine. A typical fuzzy rule is given as

    IF X is SLOW AND/OR Y is MIDDLE THEN Z is Fast

Where X and Y are input variable, Z is output variable, SLOW, MIDDLE, and

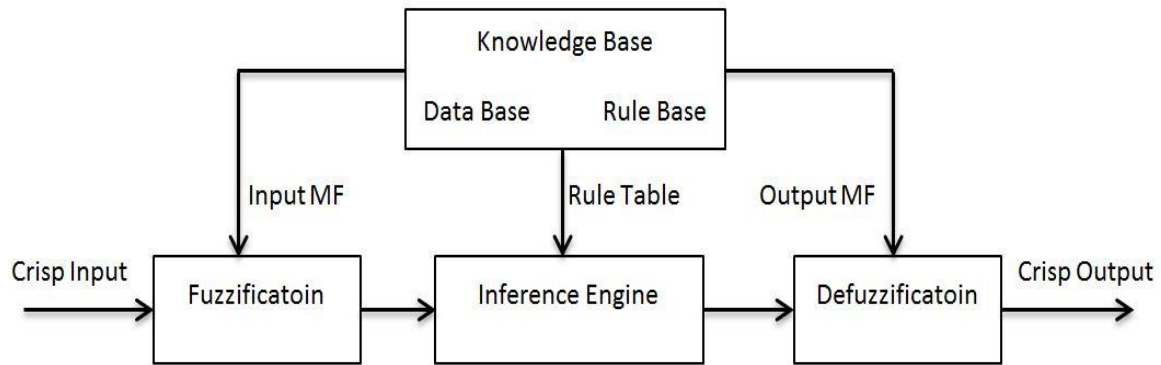FAST are fuzzy sets, AND and OR are fuzzy operators.

Figure 3.5: Basic structure of fuzzy logic controller.

2. Fuzzification

Fuzzification is the process in which the crisp input value is converted into

fuzzy number by using the input membership function.

3. Inference engine

Fuzzy inference engine is the process that relates input fuzzy sets to output

fuzzy sets using if-then rules and fuzzy operators to drive a reasonable output

fuzzy value. There are number of inference systems like Mamdani, Lusing

Larson, and Sugeno.

4. Defuzzification

Defuzzification converts the fuzzified output value to crisp control value

using the output membership function. The most famous defuzzification methods

are Center of area, Height, Mean of maxima, and Sugeno.

3.2.3 Fuzzy Logic Principle

Fuzzy controller block diagram is shown in figure 3.6. There are two input signal to the fuzzy controller, the error signal E and the derivative of error which represents the change in error signal CE. The controller output is U signal. The controller observes the loop error signal and correspondingly changes the output U so that the actual output signal matches the reference or commanded signal.
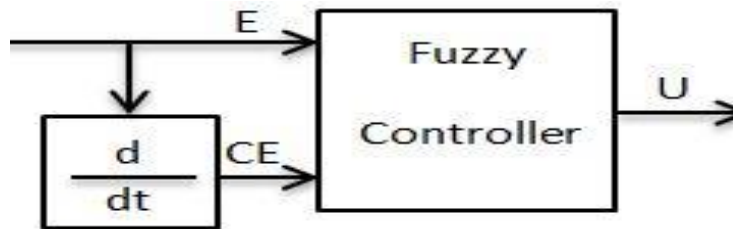

Figure 3.6: Fuzzy control system.

Figure 3.7 demonstrates the principle of two control rules with the Mamdani inference method and Height defuzzification method. The two rules are given as follow

Rule 1: IF E = ZE AND CE = NS THEN U = NS

Rule 2: IF E = PS AND CE = NS THEN U = ZE

Where E and CE are the input Fuzzy Variables, U is the output fuzzy variable, and ZE, PS, and NS are the corresponding fuzzy sets represented by triangular membership functions.

For the given rule base, the fuzzification process for the crisp input variable E is mapped by ZE and PS MFs. The output is μ_1 when referred to ZE MF in rule-1, and μ_1' when referred to PS MF in rule-2. Same for crisp input variable CE, the output is μ_2 when referred to NS MF in rule-1 and μ_2' when referred to NS MF in rule-2.
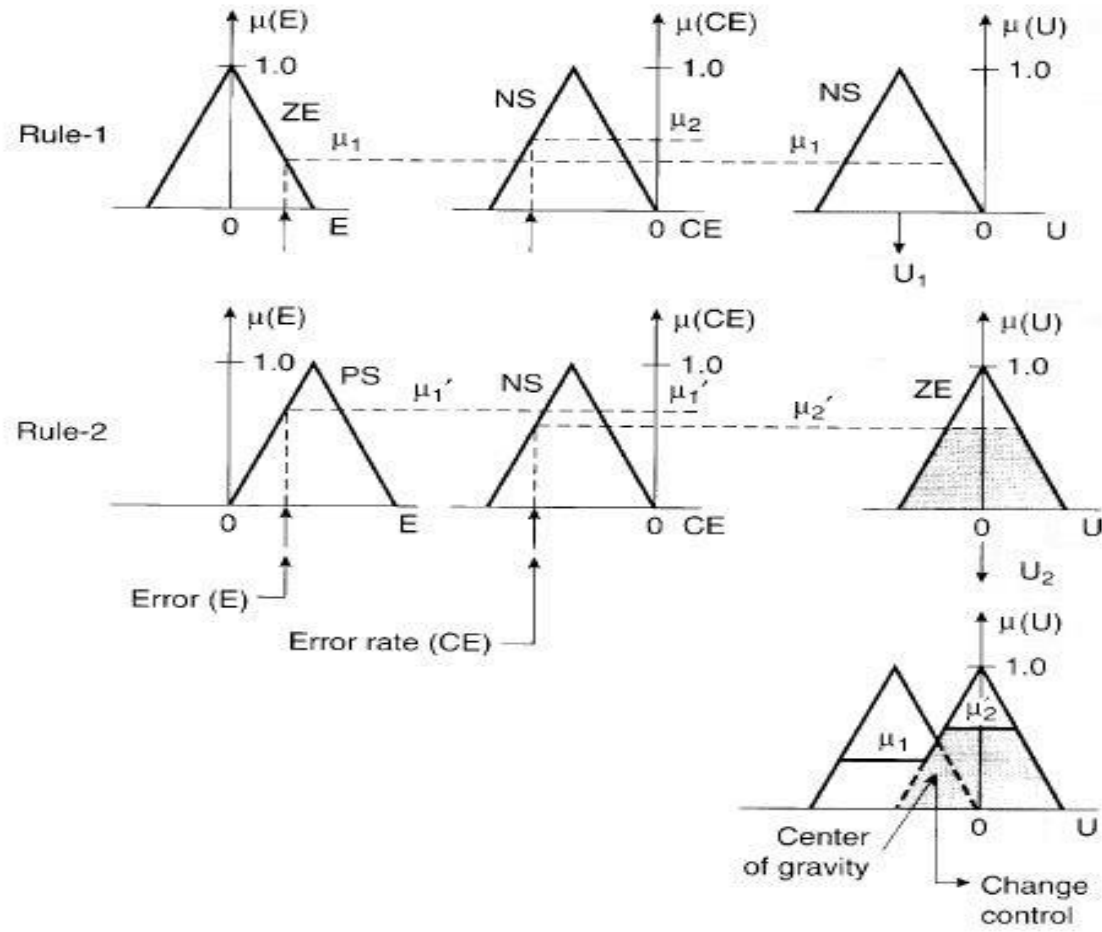
Figure 3.7: Two fuzzy rules of motor speed control [20].

Once the inputs have been fuzzified, the fuzzy operator is applied to each part of

the antecedent of the rule to get the degree of fulfillment DOF. In the above tow rules the

AND (MIN) operator is specified. Therefore, in rule1 between two values, $\mu 1$ and $\mu 2$, the

result DOF1 is $\mu 1$. Same for the rule2 between two values, $\mu 1'$ and $\mu 2'$, the result DOF2

is $\mu 2'$.

The inference step helps to evaluate the consequent part of a rule. In rule1 the

output NS membership function is truncated at the value $\mu 1$ and in rule2 the output ZE

membership function is truncated at the value $\mu 2'$. These two outputs are combined

33

together using the OR (MAX) operator to give final fuzzy output as shown at the bottom of the figure.

Finally, the fuzzy output converted to crisp output by using the Height defuzzification method. In this method the defuzzification consider only the height of each contributing MF at the mid-point of the base [20]. The output crisp value is expressed as

$$U = \frac{\sum_{l=1}^{n} z_i \mu_{out}(z_i)}{\sum_{l=1}^{n} \mu_{out}(z_i)} \quad \dots\dots\dots\dots\dots\dots\dots\dots\dots\dots\dots\dots \quad (3.5)$$

3.3. Hybrid Speed Controller

To combine the advantages of both fuzzy logic controller and conventional controllers, a hybridization of fuzzy logic and conventional controllers is proposed. The hybrid system work as a single controller with the utilization of indirect field oriented control to control the speed of squirrel cage induction motor. There are two input signals to the fuzzy controller, the error signal E and the derivative of the error which represents the change in error signal CE. The output signal U of FLC represents a new error signal that feed to PID controller. The controller observes the loop error signal and correspondingly changes the output U so that the actual output signal matches the reference or commanded signal. Some particular features that appear with conventional controllers such as overshoot and undershoot will be eliminated with the implementation of this model. Also this hybrid controller provides higher levels of stability against load variations.

3.3.1 Design Methodology

1. Identify the input and output variables of fuzzy control system.

2. Define the universe of discourse of the input and output variables.

3. Formulate the fuzzy sets and select the corresponding MF shape of each.

4. Build the fuzzy rules table. This step and the previous one are the main design steps, which need intuition and experience about the process.

5. Define the gain values of conventional controllers.

6. Simulate the system and iterate the gain values, fuzzy sets and rule table until the performance is optimized.

3.3.2 Proposed Model for Induction Motor Speed Controller

The block diagram of proposed hybrid speed controller system for a vector control drive system is shown in figure 3.8. The two input variables of fuzzy system are the motor speed error E and change in error CE. The speed error and change in error are expressed as follow

$$E = \omega_{ref} - \omega_{act} \ \dots\dots\dots\dots\dots\dots\dots\dots\dots \ (3.6)$$

$$CE = \frac{dE}{dt} \dots\dots\dots\dots\dots\dots\dots\dots\dots\dots \ (3.7)$$

Whereas, the controller output variable is T_e^* which represents the torque reference for IFOC. The controller observes the speed loop error signal and correspondingly changes the output so that the actual speed ω_{act} matches the reference speed ω_{ref}.
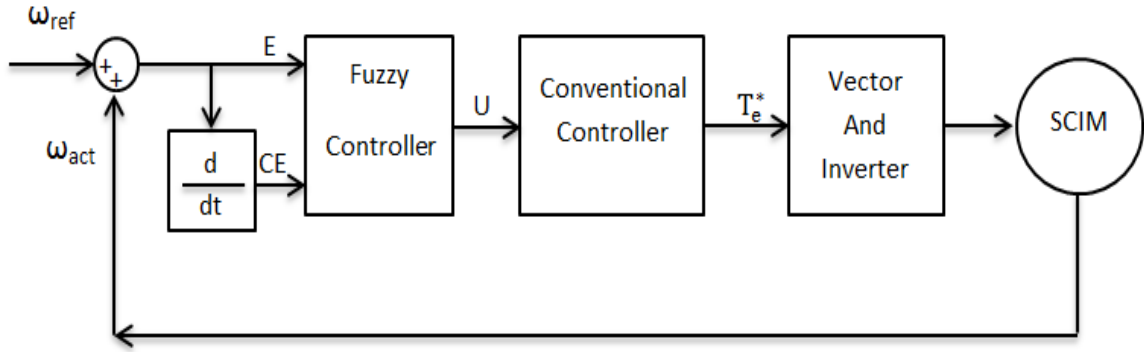
Figure 3.8: Proposed hybrid controller that combines fuzzy logic controller with conventional controller to drive SCIM with the use of vector control.

The design of fuzzy system requires the choice of fuzzy sets and membership functions. The proposed fuzzy sets (linguistic definition) are defined as follow:

PVB = Positive Very Big   PB = Positive Big   PM = Positive Medium

PS = Positive Small   Z = Zero   Ns = Negative Small

NM = Negative Medium   NB = Negative Big   NB = Negative Very Big

There are seven membership functions for both error E and change in error CE, and nine membership functions for output U as shown in figure 3.9. All membership functions should be chosen such that they cover the whole universe of discourse. To achieve finer control, the membership functions near zero should be made narrow and wider at regions away from zero to provide faster response to the system.
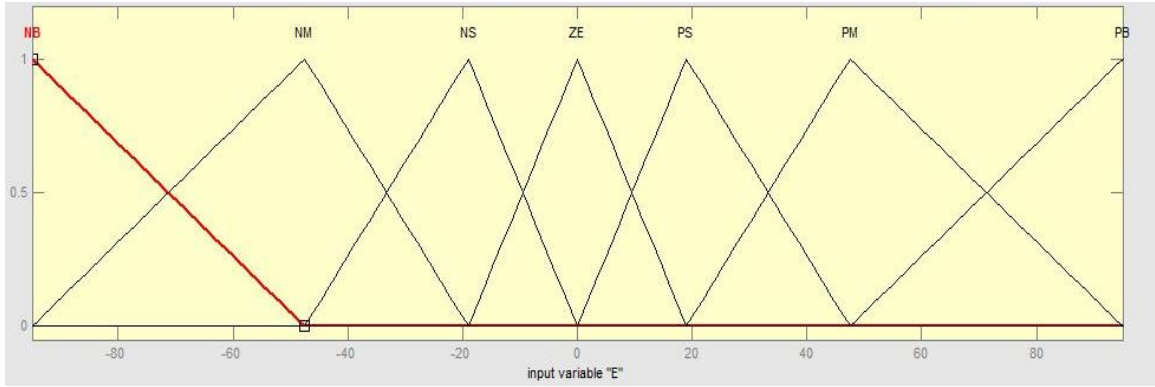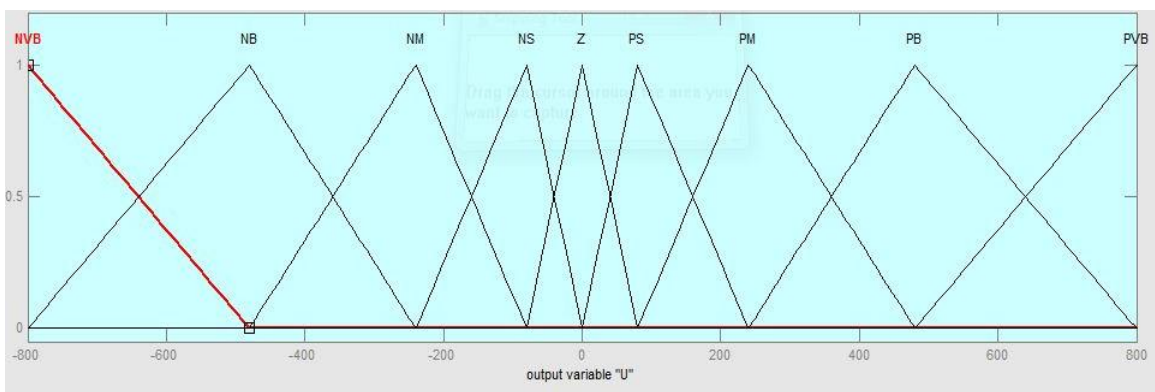
(a)
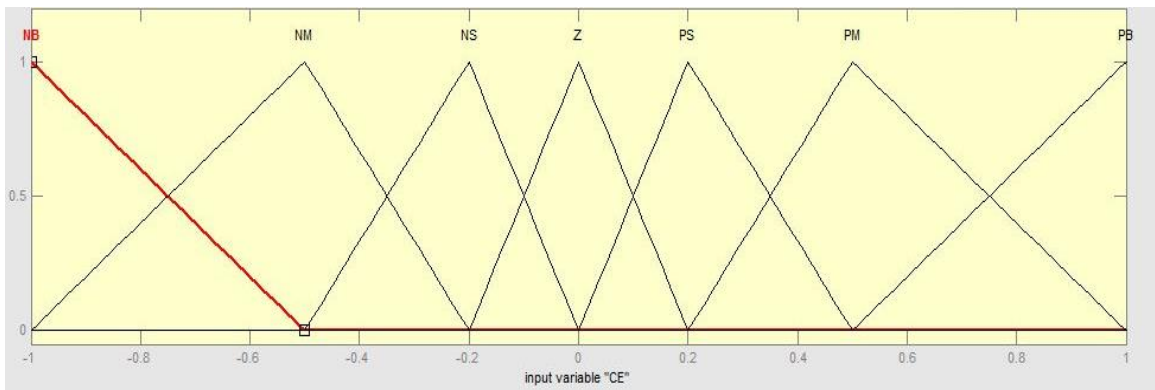
(b)

Figure 3.9: Membership functions for fuzzy speed controller (a) Error, (b)

change in error, (c) Output control signal.

The most important step in designing fuzzy system is the design of the rule base. It consists of a number of fuzzy IF-THEN rules that define the behavior of the system. Table 3.1 shows the corresponding rule table for the proposed fuzzy control system. The top row of the matrix indicates the fuzzy sets of the error variable E and the left column indicates the change in error variable CE and the output variable U is shown in the body of the matrix.

CE \ E	NB	NM	NS	Z	PS	PM	PB
NB	NVB	NVB	NVB	NB	NM	NS	Z
NM	NVB	NVB	NB	NM	NS	Z	PS
NS	NVB	NB	NM	NS	Z	PS	PM
Z	NB	NM	NS	Z	PS	PM	PB
PS	NM	NS	Z	PS	PM	PB	PVB
PM	NS	Z	PS	PM	PB	PVB	PVB
PB	Z	PS	PM	PB	PVB	PVB	PVB

Table 3.2: Fuzzy rule base table to control the speed of induction motor.

CHAPTER 4

SIMULINK MODEL AND RESULTS

Computer modeling and simulation is widely used to study the behavior of

proposed system and to decide whether the new control design processes are valid in

order to avoid the mistakes early in simulations before actual real implementation.

Among several simulation software packages, SIMULINK is one of the most powerful

techniques for simulating dynamic systems due to its graphical interface and simplicity.

SIMULINK uses MATLAB as a tool for mathematical purposes which further enhance

the modeling process. In the nest few sections, the control scheme will be presented.

4.1.   Simulink Model of Controller Scheme

A complete SIMULINK diagram of proposed control system for squirrel cage

induction motor is shown in figure 4.1. The induction motor used in this simulation is a

50 Hp, 460 V, 60 Hz, squirrel cage having the parameters listed in table 4.1. The

induction motor stator is fed by a current controlled three-phase inverter bridge. The

stator currents are regulated by hysteresis regulator which generates inverter drive signals

for the inverter switches to control the induction motor. The motor torque is controlled by

the quadrature-axis current component I_q^{e*} and the motor flux is controlled by direct-axis

current component I^{e*}. The motor speed is regulated by a hybrid control which produces

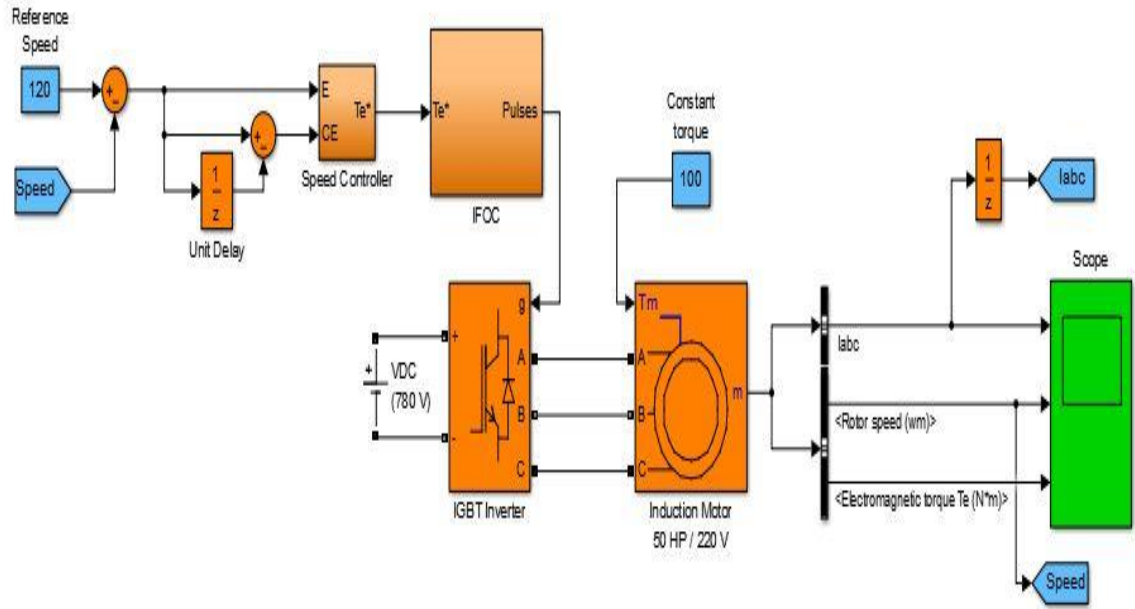the required torque current component signal I_q^{e*}.

Figure 4.1: Complete SIMULINK model of speed controller system for three-phase squirrel cage induction motor.

Parameter	Symbol	value	Unit
Stator resistance	RS	0.087	Ω
Rotor resistance	Rr	0.228	Ω
Mutual inductance	Lm	34.7	mH
Stator inductance	LIs	0.8	mH
Rotor inductance	LIr	0.8	mH
Inertia	J	1.662	kg.m^2
Friction factor	F	0.1	N.m.s
Pole pairs	P	2	()

Table 4.1: A list of induction motor parameters with values based on predefined model in MATLAB.

4.1.1   Field Oriented Control Sub-Blocks

The indirect field oriented control algorithm has been simulated in MATLAB as shown in figure 4.2. All sub blocks will be reviewed in the next coming sections.
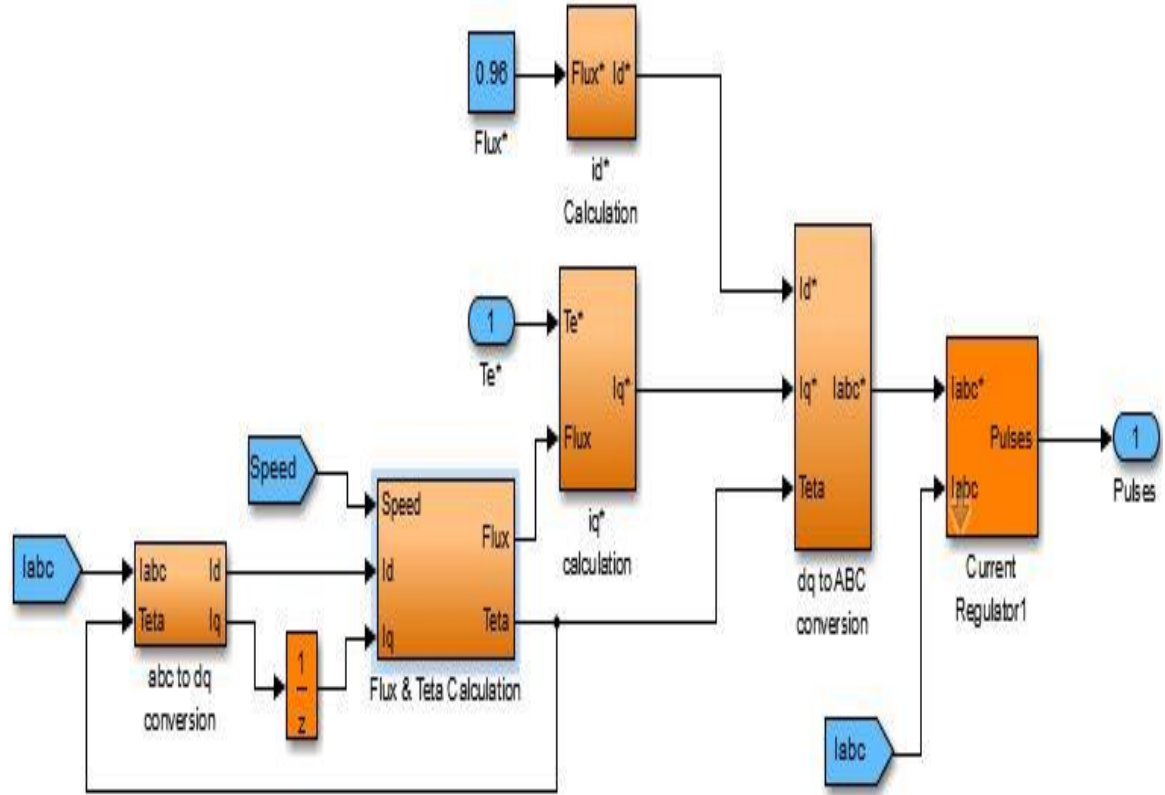

Figure 4.2: Field oriented control SIMULINK model.

4.1.1.1   Forward Clarke and Park Transformation

Figure 4.1 shows the SIMULINK model that converts the I_{as}, I_{bs}, and I_{cs} phase variables into I^e and I_q^e current components in rotating reference frame d^e-q^e. Equations (2.7) and (2.9) represent the mathematical relationship between the three-phase variables I_{as}, I_{bs}, and I_{cs} and current components I^e and I_q^e. The simulation is done by entering

stator currents to the mux and applying the mathematical operation using function block
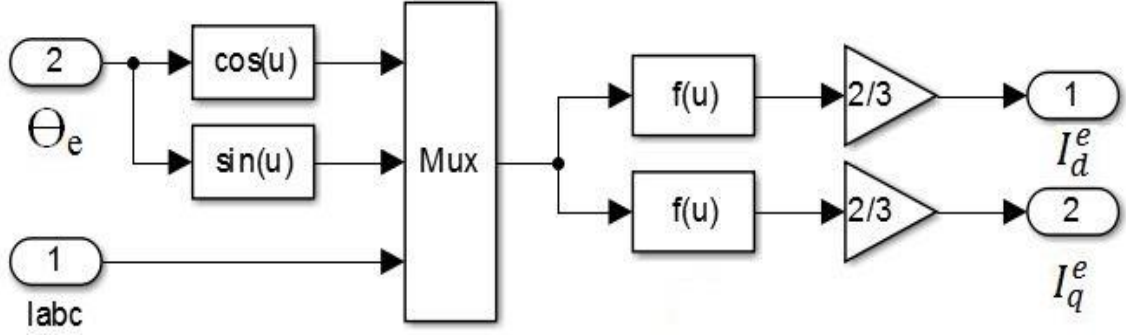
parameters provided by MATLAB.

Figure 4.3: Forward Clarke and Park transformations SIMULINK model.

In figure 4.3, we define the following:

- Θ_e represents the angle between d^e-axis and rotor flux vector.

- I_{abc} represents the three-phase stator currents I_{as}, I_{bs}, and I_{cs}.

- I_d^e and I_q^e represents the stator current components in rotating reference frame.

4.1.1.2   Rotor Flux and Angle Calculation

Knowledge of the rotor flux vector magnitude and position is key information for

field oriented control of the three-phase induction motor. The SIMULINK model of

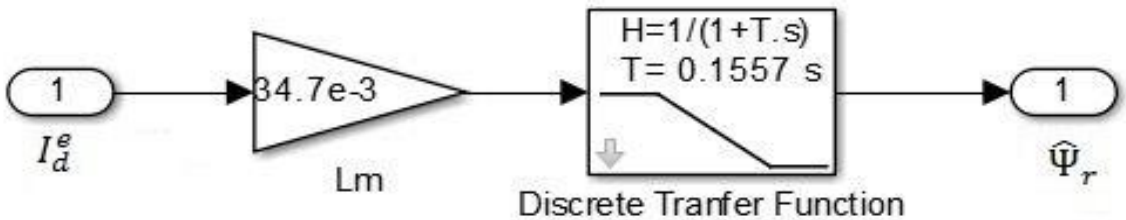equations (2.19) and (2.17) are shown in figure 4.4 and 4.5 respectively.

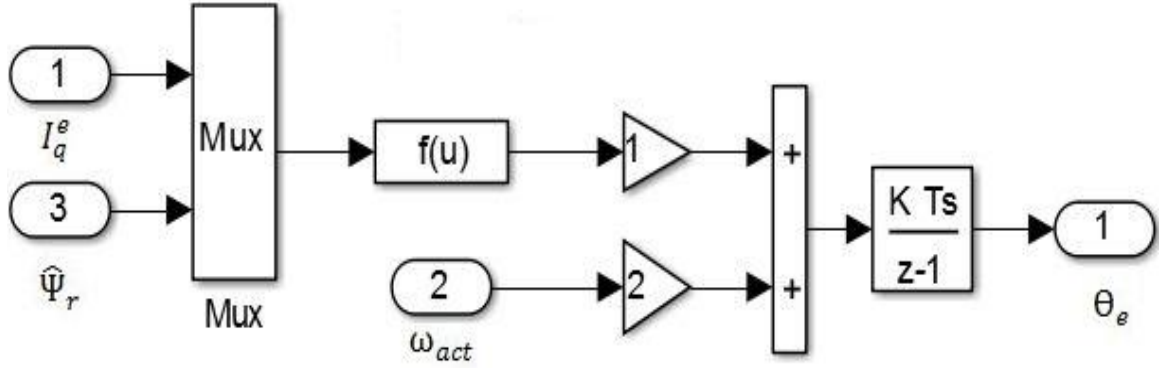Figure 4.4: Rotor flux magnitude calculation.

Figure 4.5: SIMULINK model to calculate rotor flux position (angle) that is necessary for transformation from stationary to rotating reference frame or vice versa.

4.1.1.3 Direct Reference Current Calculation

The stator direct-axis current reference I^{e*} can be obtained using equation (2.22). Figure 4.6 shows the SIMULINK model of the two equations.
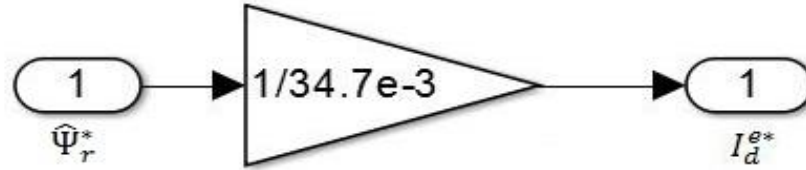

Figure 4.6: SIMULINK model to calculate the direct current reference component I^{e*}.

In figure 4.6, we have

- $\hat{\Psi}_r^*$ represents the reference flux value.

- I^{e*} represents direct current reference component.

4.1.1.4 Quadrature Reference Current Calculation

The SIMULINK model shown in figure 4.6 used to obtain the stator quadrature reference current I_q^{e*} by using equations (2.19) and (2.21).
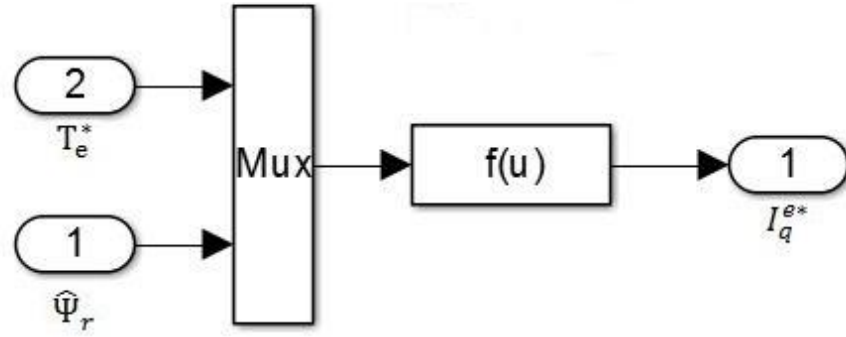
43

Figure 4.7: SIMULINK model to calculate quadrature current reference component I_q^{e*}.

In figure 4.7, we have

- T_e^* represents the reference torque obtained from speed controller.

- I_q^{e*} represents the quadrature reference current component.

4.1.1.5 Inverse Clarke and Park Transformation

The inverse transformation SIMULINK model is shown in figure 4.2. This block uses equations (2.8) and (2.10) to perform the conversion of the I_d^e and I_q^e stator current components in rotating reference frame back I_{as}, I_{bs}, and I_{cs} in stationary reference frame.
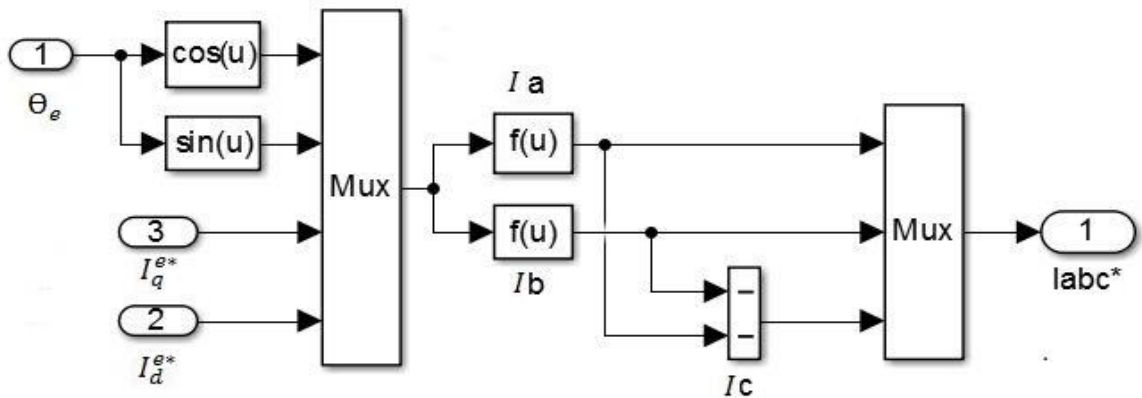

Figure 4.8: SIMULINK model to convert current components in rotating frame to three-phase currents in stationary frame.

4.1.1.6   Current Regulator

The current regulator shown in figure 4.8 is a feedback current control method where the motor current tracks the reference current within hysteresis band. In this method the reference current is compared to actual motor current. As a result, six pulses are generated to control the switches of inverter in order to provide the motor with desired magnitude and frequency current signals.
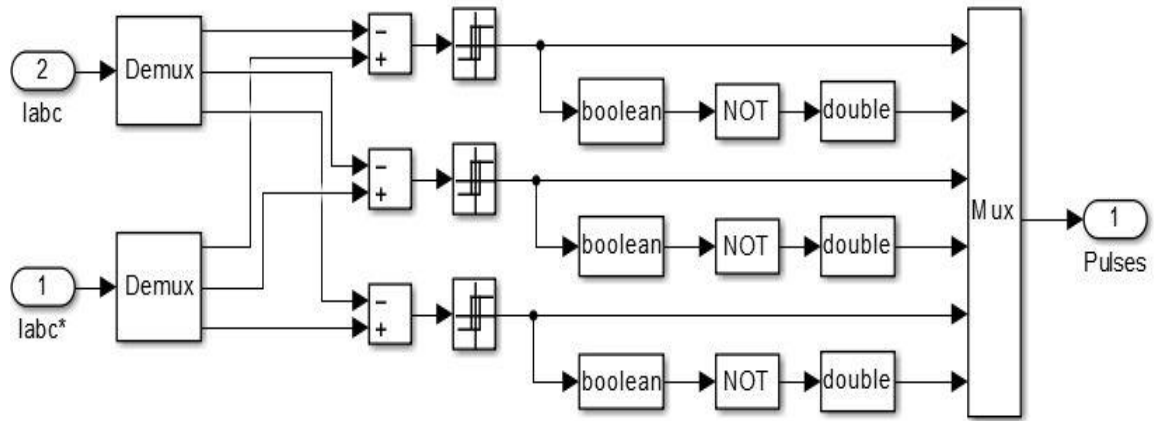
Figure 4.9: SIMULINK model of current regulator.

4.1.2   Speed Controller Sub-Block

The speed controller block contains fuzzy controller and conventional controller. The fuzzy and conventional controllers developed in MATLAB using fuzzy logic toolbox and PID regulator respectively. The SIMULINK model for speed controller is shown in figure 4.9. This model has the speed error and change in error as input. The output signal from the model is the torque reference value which is then provided to FOC block as input.

Figure 4.10: SIMULINK model of speed controller.

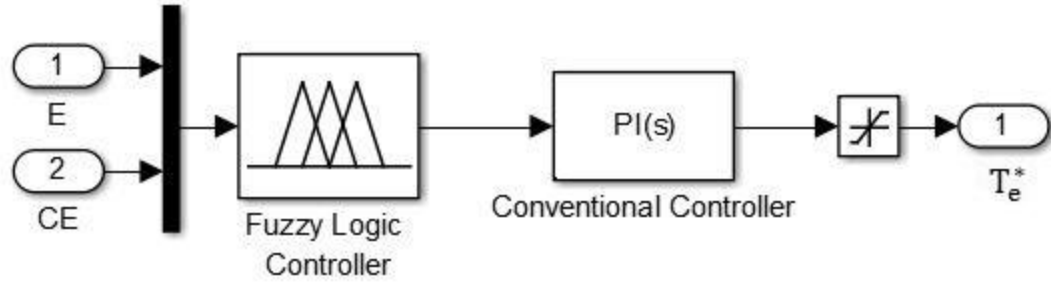In figure 4.10, we have

E and CE represent error and change in error.

T_e^* represents reference torque.

4.2.   Results and Discussion

In this section, we present simulation results of the proposed speed controllers using MATLAB/SIMULINK and analyze them against the performance of three-phase squirrel cage induction motor. The effectiveness and robustness of the developed conventional PI controller and three proposed hybrid PI-, PD-, PID-Fuzzy speed controllers are evaluated under various operating conditions. The transient performances of all controllers are investigated while varying the reference speed and load torque values.

4.2.1   Fixed Reference Speed and Varying Load Torque for all Controllers

The reference speed for all controllers was fixed at 120 rad/sec and reference load torque was varying from 0 to 200 by 50 N.m steps. The computational time interval for conventional PI controller model was fixed at 7 seconds while for hybrid controller

model it was fixed at 1 second. The response curves for PI speed controller and PI-, PD-, PID-Fuzzy speed controllers are extracted as shown in figures 4.11 through 4.14 respectively. The values of the different performance parameters such as rise time (t_r), settling time (t_s), peak overshoot (M_p), and steady state error (e_{ss}) of each controller are shown in table 4.1. According the results, it can be said that PID-Fuzzy has fast transient response and less overshoot than other controllers.

Figure 4.11: Speed response curve of SCIM at 100 N.m load torque and 120 rad/sec reference speed using PI controller.
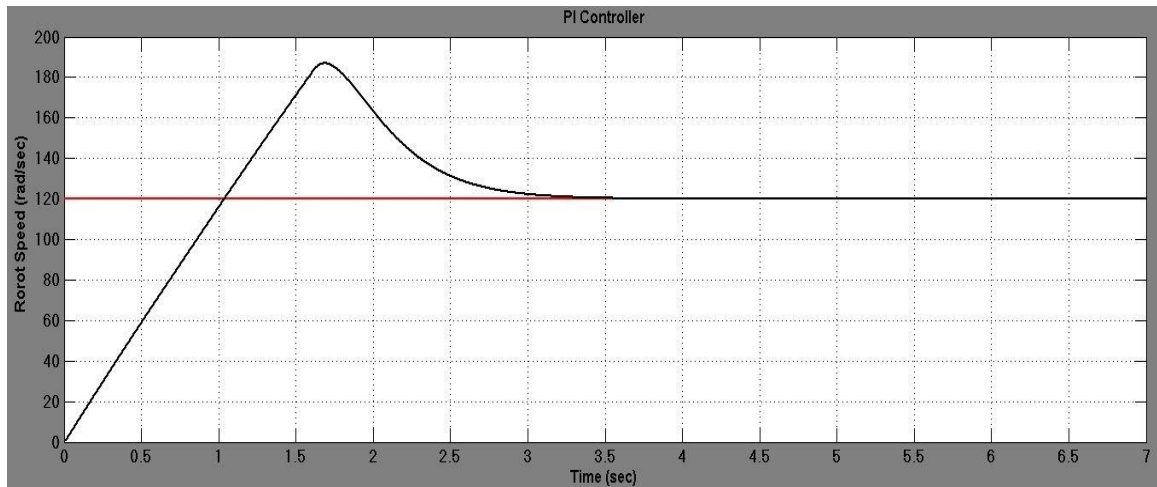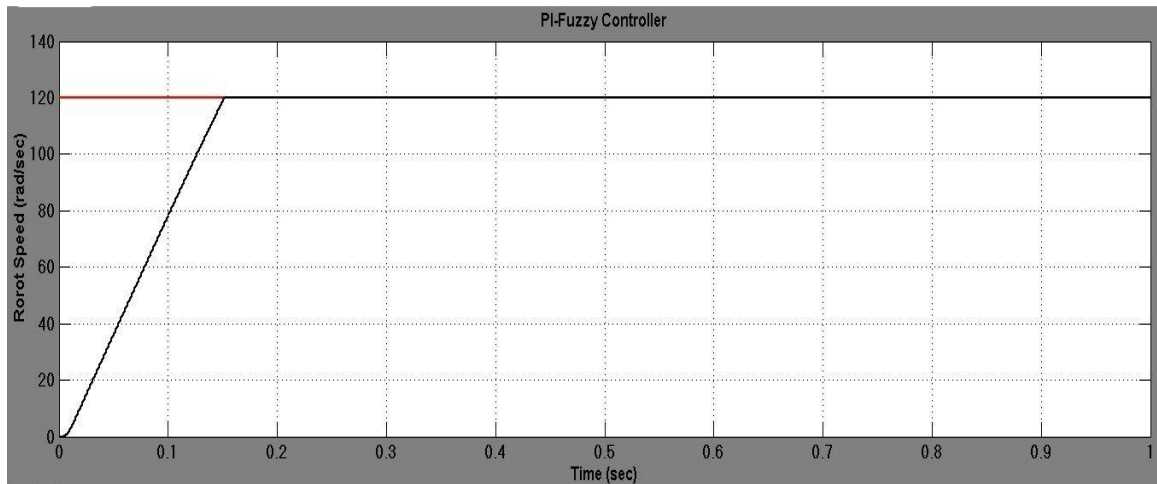

Figure 4.12: Speed response curve of SCIM at 100 N.m load torque and 120 rad/sec reference speed using PI-Fuzzy controller.
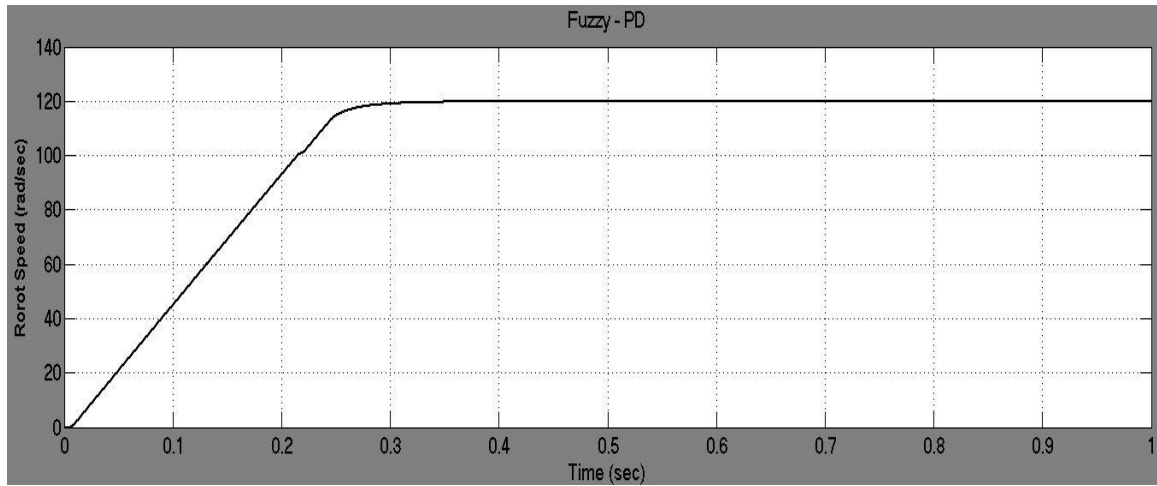
Figure 4.13: Speed response curve of SCIM at 100 N.m load torque and 120 rad/sec reference speed using PD-Fuzzy controller.
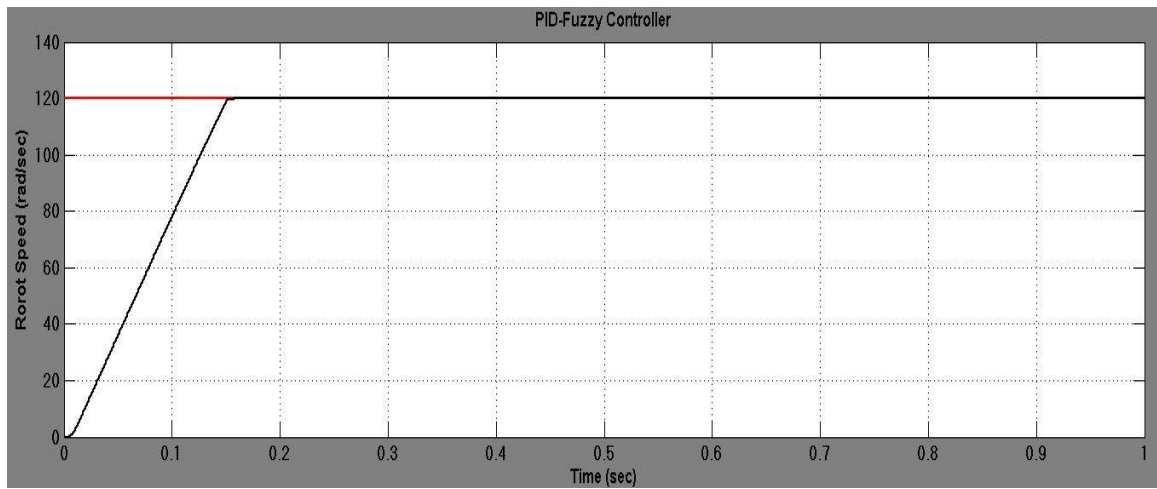

Figure 4.14: Speed response curve of SCIM at 100 N.m load torque and 120 rad/sec reference speed using PID-Fuzzy controller.

Load (N.m)	Controller	t_r (sec)	t_s (sec)	M_p	e_{ss}
0	PI	0.5439	2.3053	45.6222	0.015
	PD-Fuzzy	0.1649	0.2246	0	0.004
	PI-Fuzzy	0.1071	0.1386	0.1423	0.1600
	PID-Fuzzy	0.1071	0.1386	0.0411	0.0460
100	PI	0.8264	2.9875	55.7523	0.005
	PD-Fuzzy	0.1815	0.2444	0	0.0570
	PI-Fuzzy	0.1146	0.1484	0.0994	0.1100
	PID-Fuzzy	0.1146	0.1484	0.0016	0.0005
150	PI	1.1171	3.7192	62.7390	0.0040
	PD-Fuzzy	0.1915	0.2563	0	0.0835
	PI-Fuzzy	0.1189	0.1539	0.0792	0.0880
	PID-Fuzzy	0.1189	0.1539	0	0.0205
200	PI	1.7215	5.2680	69.8961	0.007
	PD-Fuzzy	0.2027	0.2698	0	0.1098
	PI-Fuzzy	0.1234	0.1598	0.0591	0.0650
	PID-Fuzzy	0.1234	0.1598	0	0.0440

Table 4.2: Performance analyses of different speed controllers for SCIM at 120 rad/sec reference speed and different load torque.

4.2.2   Fixed Load Torque and Step Change in Reference Speed

The dynamic performances of the PI and PID-Fuzzy controllers are analyzed by applying 100 N.m torque load and step change in reference speed, 60 rad/sec to 120 rad/sec, at 3rd second interval time for PI controller and PID-Fuzzy controller. Figure 4.15 and 4.16 show the simulation results of both controllers. In these figures, the red line represents the reference speed and black line represents the response curve. By analyzing figure 4.15, the motor speed in PI controller following the reference speed (60 rad/sec) until a step change in reference speed is applied to the motor at 3rd second interval time.
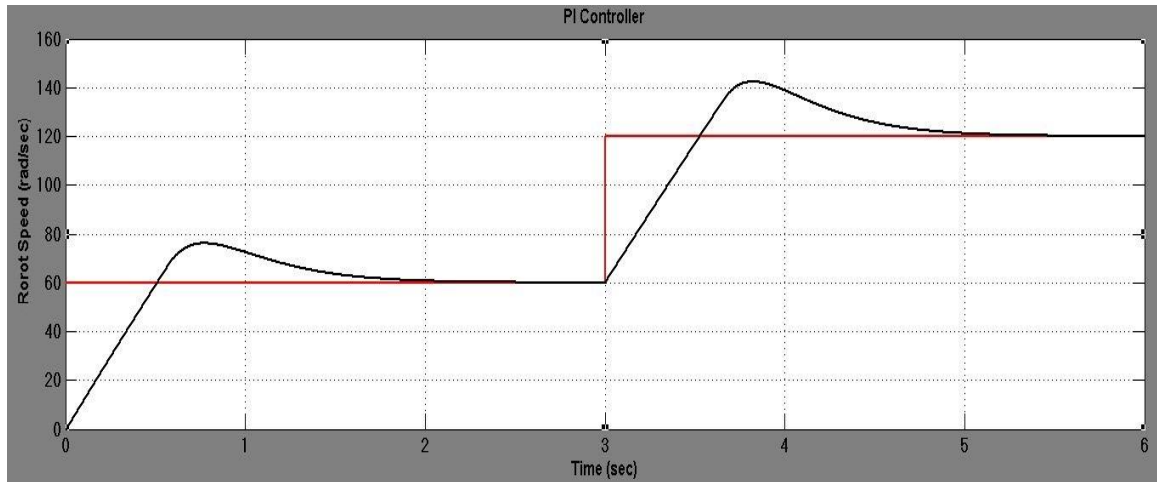
Figure 4.15: Speed response curve of SCIM at 100 N.m load torque and 60 to 120 rad/sec step change in reference speed using PI controller.
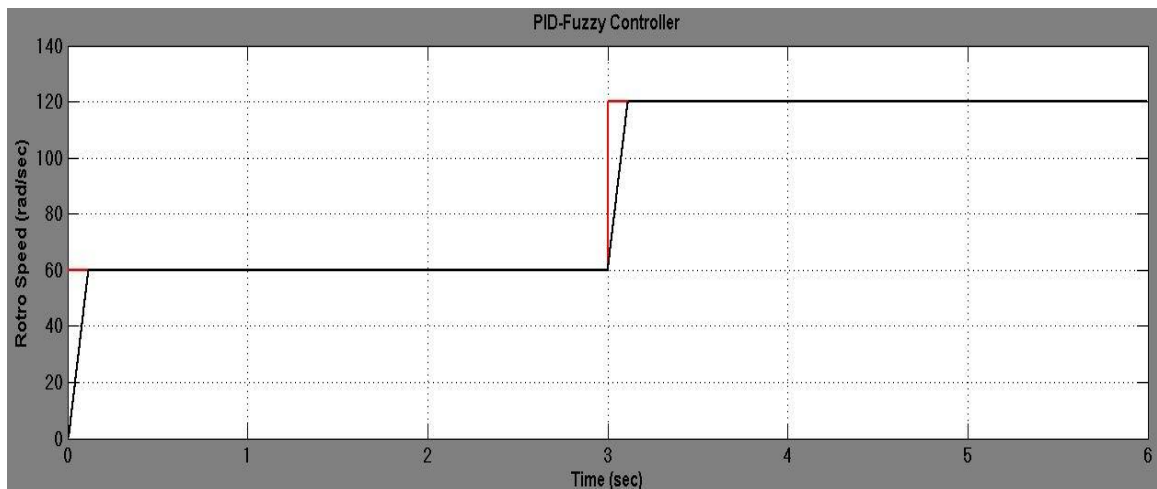
Figure 4.16: Speed response curve of SCIM at 100 N.m load torque and 60 to 120 rad/sec step change in reference speed using PID-Fuzzy controller.

We can easily notice that the motor speed response curve shows overshoot = 22.3 and deviation from reference speed that runs for 2.5 second and then return to the desired speed. In the case of PID-Fuzzy controller as shown in figure 16, the speed response doesn't show any overshoot and the deviation run for 0.08 second which is short time compared to PI controller.

50

4.2.3   Fixed Reference Speed and Step Change in Load Torque

In the third step of simulation studies, the dynamic performances of the PI and PID-Fuzzy controllers are analyzed by applying step change in load torque, 50 N.m to 200 N.m, at 3rd second interval time for PI controller and PID-Fuzzy controller. Figure 4.17 and 4.18 show the simulation results of both controllers.

From figure 4.17, it is clear that the motor speed in PI controller is following the speed reference (120 rad/sec). It is also obvious that the response curve shows undershoot and deviation when a step change in load torque is applied to the motor at 3 second interval time. The deviation continues for 1.6 seconds and then returns to the desired speed reference. When using PID-Fuzzy controller the speed response as shown in figure 4.18 doesn't show any undershoot or deviation except small change in steady state error.

Figure 4.17: Speed response curve of SCIM at 120 rad/sec reference speed and 50 to 200 N.m step change in load torque using PI.

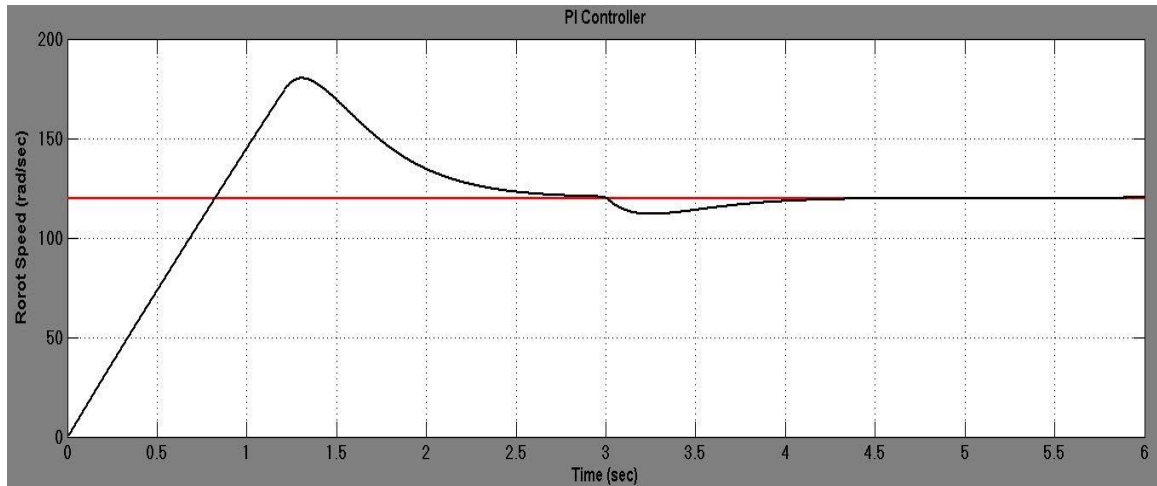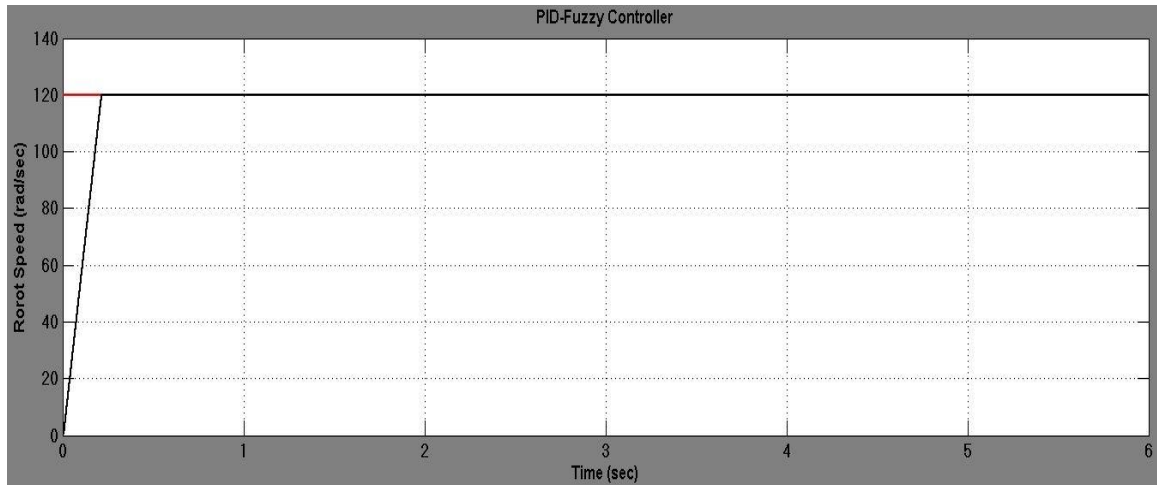Figure 4.18: Speed response curve of SCIM at 120 rad/sec reference speed and 50 to 200 N.m step change in load torque using PID-Fuzzy controller.

CHAPTER 5

CONCLUSION AND FUTURE WORK

This thesis has successfully presented a hybrid PID-Fuzzy system for controlling a three-phase squirrel cage induction motor. Hybridization of fuzzy logic and conventional controllers is used as a single controller. Additionally, the indirect field oriented control is utilized in the proposed hybrid system to solve the induction motor coupling effects problem that makes the system response sluggish and easily prone to instability.

PI, PI-, PD-, and PID-fuzzy were designed and simulated in MATLAB/Simulink. The performance and robustness of all controllers have been evaluated under realistic operating conditions. Furthermore, a comparative study of the different control schemes has been completed using the performance significant measures such as rise time (t_r), peak overshoot (M_p), settling time (t_s), and steady state error (E_{ss}).

Based on simulation results verification, it is concluded that dynamic response characteristics with the hybrid PID-Fuzzy controller take less time to settle and do reach the final steady state value especially when compared with the PI conventional controller. Also, the hybrid controller shows better robustness during the transient period and during the sudden load changes compared with PI controller.

In conclusion, I demonstrated that the proposed hybrid PID-Fuzzy speed controller for closed loop operation of the induction motor drive system has improved

performance over the PI conventional controller and that it gives better speed response and shows higher levels of robustness and effectiveness.

Future work should include applying the proposed method to real time system and conduct full analysis of other power quality issues such as harmonic distortion, voltage imbalance, and power factor improvements. Additionally, system protection should take into consideration both under and over voltage conditions. Finally, it is essential to comment on the fact that induction motor working at rated flux will give optimum transient response, however, at lighter loads, excessive core loss can occur resulting in a very low efficiency. Therefore, future work should improve the motor efficiency by controlling the flux and thus allow for obtaining a balance between the copper and iron losses.

BIBLIOGRAPHY

[1] Ashok Kusagur, Shankarappa Fakirappa Kodad, and Sanker Ram, "Modelling & Simulation of an ANFIS controller for an AC drive," *World Journal of Modelling and Simulation*, vol. 8, no. 1, pp. 36-49, March 2011.

[2] (2012, April) http://machinedesign.com/. [Online]. http://machinedesign.com/motorsdrives/difference-between-ac-induction-permanent-magnet-and-servomotor-technologies

[3] Amit Mishra and Zaheeruddin, "Design of Speed Controller for Squirrel-cage Induction Motor using Fuzzy logic based Techniques," *International Journal of Computer Applications*, vol. 58, no. 22, pp. 10-18, November 2012.

[4] Pabitra Kumar Behera, Manoj Kumar Behera, and Amit Kumar Sahoo, "Comparative Analysis of scalar & vector control of Induction motor through Modeling & Simulation," *INTERNATIONAL JOURNAL OF INNOVATIVE RESEARCH IN ELECTRICAL, ELECTRONICS, INSTRUMENTATION AND CONTROL ENGINEERING*, vol. 2, no. 4, pp. 1340-1344, April 2014.

[5] Ch Chengaiah and Silva Prasad, "Performance of Inductoin Motor Drive by Indirect vector controlled method using PI and Duzzy Controllers," *International Journal of Science, Environment*, vol. 2, no. 3, pp. 475-469, 2013.

[6] Sharda Patwa, "CONTROL OF STARTING CURRENT IN THREE PHASE INDUCTION MOTOR USING FUZZY LOGIC CONTROLLER," *International Journal of Advanced Technology in Engineering and Science*, vol. 1, no. 12, pp. 27-32, December 2013.

[7] Ashok Kusagur, S. F. Kodad, and B. V. Sankarram, "Modelling of Induction Motor & Control of Speed Using Hybrid Controller Technology," *Journal of Theoretical and Applied Information Technology*, 2009.

[8] Amanulla and Manjunath Prasad, "Artificial Neural Network Based Speed and Torque Control of Three Phase Induction Motor," *International Journal of Science and Research (IJSR)*, vol. 2, no. 8, pp. 462-465, August 2013.

[9] Fatih Korkmaz, Ismail Topaloglu, and Hayati Mamur, "FUZZY LOGIC BASED DIRECT TORQUE CONTROL OF INDUCTION MOTOR WITH SPACE VECTOR MODULATION," *International Journal on Soft Computing, Artificial Intelligence and Applications*, vol. 2, pp. 5-6, December 2013.

[10] S. Senthilkumar and S. Vijayan, "Simulation of High Performance PID Controller

for Induction Motor Speed Control with Mathematical Modeling".

[11] Mostafa A. Hamood, Waleed F. Faris Marwan A. Badran, "Fuzzy Logic Based Speed Control System for Three Phase Induction Motor," *EFTIMIE MURGU*, pp. ISSN 1453 - 7397, January 2013.

[12] Nitin Goel, P. R. Sharma, and Suman Bala, "PERFORMANCE ANALYSIS OF SPWM INVERTER FED 3-PHASE INDUCTION MOTOR DRIVE USING MATLABSIMULINK," *International Journal of Advanced Technology in Engineering and Science*, vol. 2, no. 6, pp. 183-193, June 2014.

[13] RAFIYA BEGUM, ZAKEER MOTIBHAI, and GIRIJA NIMBAL, "Induction Motor Modelling Using Fuzzy Logic (Fl) Speed Controller," *Journal of Computer and Mathematical Sciences*, vol. 4, no. 2, pp. 80-134, April 2013.

[14] Shelby Mathew and Bobin K. Mathew, "Direct Torque Control of Induction Motor Using Fuzzy Logic Controller," *International Journal of Advanced Research in Electrical, Electronics and Instrumentation Engineering*, vol. 2, no. 1, pp. 386-394, December 2013.

[15] F. Blaschke, "The Principle of Field Orientation as Applied to the New Transvector Closed Loop Control Systems for Rotating Machines," *Siemens Review*, vol. 39, no. 5, pp. 217-220, 1972.

[16] Ashish Chourasia, Vishal Srivastava, Abhishek Choudhary, and Sakshi Praliya, "Comparison study of Vector Control of Induction Motor Using Rotor Flux Estimation by Two Different Methods," *International Journal of Electronic and Electrical Engineering*, vol. 7, no. 3, pp. 201-206, 2014.

[17] Andrzej M. Trzynadlowski, *The Field Orientation Principle in Control of Induction Motors*, 1st ed., Thomas A. Lipo, Ed. Massachusetts, USA: Kluwer Academic, 1994.

[18] Rakesh Singh Lodhi and Payal Thakur, "Performance & Comparison Analysis of Indirect Vector Control of Three Phase Induction Motor," *International Journal of Emerging Technology and Advanced Engineering*, vol. 3, no. 10, pp. 716-724, Octorber 2013.

[19] Andrzej M. Trzynadlowski, *Contorl of Induction Motors*, David J. Irwin, Ed. San Diego, USA: A Harcourt SCience and Technology Company, 2001.

[20] Bemal K. Bose, *Modren Power Electronics and Ac Drives*, 1st ed., Bernard Goodwin, Ed. USA: Prentice Hall, Inc., 2002.

[21] Bilal Akin and Manish Bhardwaj, "Sensored Field Oriented Control of 3-Phase

Induction," Texas Instruments, Dallas, Application Report SPRABP8, 2013.

[22] "Field Orientated Control of 3-Phase AC-Motors," Texas Instruments Europe, BPRA073, 1998.

[23] Surajit Chattopadhyay, Madhuchhanda Mitra, and Samarjit Sengupta, *Electric Power Quality*. NewYork, USA: Springer Science, 2011.

[24] Hamid Khan, "Field Oriented Control," Renesas, 2008.

[25] Ashutosh Mishra and Prashant Choudhary, "Speed Control Of An Induction Motor By Using Indirect Vector Control Method," *International Journal of Emerging Technology and Advanced Engineering*, vol. 2, no. 12, pp. 144-150, December 2012.